

**INVESTIGATIVE COMPARISON OF TANK AND RECOVERED ASPHALT
SAMPLES THROUGH PHYSICAL PERFORMANCE TESTING AND CHEMICAL
ANALYSIS**

by

MICHAEL SOMUAH

A thesis submitted to the Department of Chemistry

in conformity with the requirements for

the Degree of Master of Science

Queen's University

Kingston, Ontario, Canada

(DECEMBER, 2016)

Copyright © MICHAEL SOMUAH, 2016.

ABSTRACT

Despite the development of improved performance test protocols by renowned researchers, there are still road networks which experience premature cracking and failure. One area of major concern in asphalt science and technology, especially in cold regions in Canada is thermal (low temperature) cracking. Usually right after winter periods, severe cracks are seen on poorly designed road networks. Quality assurance tests based on improved asphalt performance protocols have been implemented by government agencies to ensure that roads being constructed are at the required standard but asphalt binders that pass these quality assurance tests still crack prematurely. While it would be easy to question the competence of the quality assurance test protocols, it should be noted that performance tests which are being used and were repeated in this study, namely the extended bending beam rheometer (EBBR) test, double edge-notched tension test (DENT), dynamic shear rheometer (DSR) test and X-ray fluorescence (XRF) analysis have all been verified and proven to successfully predict asphalt pavement behaviour in the field. Hence this study looked to probe and test the quality and authenticity of the asphalt binders being used for road paving. This study covered thermal cracking and physical hardening phenomenon by comparing results from testing asphalt binder samples obtained from the storage ‘tank’ prior to paving (tank samples) and recovered samples for the same contracts with aim of explaining why asphalt binders that have passed quality assurance tests are still prone to fail prematurely.

The study also attempted to find out if the short testing time and automated procedure of torsion bar experiments can replace the established but tedious procedure of the EBBR.

In the end, it was discovered that significant differences in performance and composition exist between tank and recovered samples for the same contracts. Torsion bar experimental data also indicated some promise in predicting physical hardening.

ACKNOWLEDGMENTS

A huge thank you to my supervisor, Dr. Simon Hesp for the privilege of working with him and learning from him, and for his continued patience, guidance and support. I would also like to thank Dr. Guojun Liu and Dr. Donal Macartney for being part of my supervisory committee.

Much gratitude goes to Ontario Ministry of Transportation (MTO), Imperial Oil Research Centre, and Natural Sciences and Engineering Research Council (NSERC) for their financial support towards this study and to summer students Amanda Rigg, Alistair Duff, Justin Kaskow, Michael Assuras, as well as my colleague Nathaniel Tetteh for assistance with data collection and sample preparation.

Finally, I'm grateful to the Almighty God, for seeing me through the completion of my thesis and to my family and friends for their prayers, love and support.

Table of Contents

ABSTRACT.....	i
ACKNOWLEDGMENTS	iii
ABBREVIATIONS AND ACRONYMS	xii
CHAPTER 1	1
INTRODUCTION	1
1.1 Overview.....	1
1.2 Composition of Asphalt	2
1.3 Separation of Components.....	3
1.4 Asphalt Behaviour	4
1.4.1 High Temperature Behaviour.....	5
1.4.2 Low Temperature Behaviour	8
1.4.3 Intermediate Temperature Behaviour	8
1.4.4 Aging Behaviour.....	9
1.5 Objectives and Scope.....	10
CHAPTER 2	11
BACKGROUND	11
2.1 Asphalt Distresses.....	11
2.1.1 Fatigue Cracking.....	12
2.1.2 Moisture Damage.....	13
2.1.3 Rutting.....	14

2.1.4 Thermal Cracking	15
2.2 Asphalt Binder Testing Procedures.....	19
2.2.1 Conventional Test Procedures	19
2.2.2 Superpave Specification Procedures	24
2.2.3 Newly Approved Test Procedures (Accepted by MTO and recently by AASHTO)	33
CHAPTER 3	39
MATERIALS & EXPERIMENTAL METHODS.....	39
3.1 Materials	39
3.1.1 Asphalt Cement Aging.....	39
3.1.2 Rolling Thin Film Oven (RTFO) Test	39
3.1.3 Pressure Aging Vessel (PAV) Test.....	40
3.1.4 Recovery of Asphalt Binder from Asphalt Core Samples	41
3.2 Dynamic Shear Rheometer (DSR) Method	43
3.2.1 High and Intermediate Temperature Tests.....	43
3.2.2 Torsion Experiments	44
3.3 Bending Beam Rheometer (BBR) Method	45
3.3.1 Extended Bending Beam Rheometer (EBBR) Method.....	46
3.4 Double-Edge Notched Tension (DENT) Test LS-299.....	47
3.5 X-Ray Fluorescence (XRF) Analysis	47
CHAPTER 4	49

RESULTS & DISCUSSION.....	49
4.1 Extended Bending Beam Rheometer (LS-308) Method.....	49
4.3 X-Ray Fluorescence (XRF) Analysis	58
4.4 Dynamic Shear Rheometer Analysis	65
4.4.1 Torsion Bar Experiments	67
CHAPTER 5	74
SUMMARY & CONCLUSION	74
REFERENCES	76

List of Figures

Figure 1.1: Annual asphalt usage in the U.S. [2]	2
Figure 1.2: Asphalt cement component [2]	4
Figure 1.3: Microscopic shot of liquid flow [2]	5
Figure 1.4: Newtonian fluid behaviour [2]	6
Figure 1.5: Pseudo-plastic flow behaviour [2]	7
Figure 1.6: Dilatant flow behaviour [2]	7
Figure 1.7: “Spring-Dashpot” model [2]	8
Figure 2.1: Fatigue (alligator) cracking [15]	13
Figure 2.2: Moisture damage (stripping) [16]	14
Figure 2.3: Rutting [20]	15
Figure 2.4: Thermal cracking of asphalt pavement [22,23]	16
Figure 2.5: Penetration test equipment [35]	21
Figure 2.6: Ring and ball apparatus [37]	22
Figure 2.7: Viscosity test apparatus [38]	23
Figure 2.8: Rolling Thin Film Oven [39,40]	26
Figure 2.9: Pressure Aging Vessel and its components [42]	27
Figure 2.10: Bending Beam Rheometer [46]	30

Figure 2.11: Schematic diagram of the BBR [47]	30
Figure 2.12: AR 2000 Dynamic Shear Rheometer [49]	32
Figure 2.13: Double Edged Notched Tension (DENT) test [59]	35
Figure 2.14: Fracture process zone and outer plastic zone of asphalt binder [61]	37
Figure 3.1: Sample preparation for RTFO test [39]	40
Figure 3.2: Sample preparation for PAV tests [42]	41
Figure 3.3: A Cole Parmer rotary evaporator [66]	42
Figure 3.4: DSR samples in silicon molds [67]	43
Figure 3.5: Preparation of BBR beams [46]	45
Figure 3.6: BBR beam ready to be tested [46]	46
Figure 4.1: Low temperature grades for tank and recovered samples from the same paving contracts.....	50
Figure 4.2: Grade loss in tank and recovered asphalt samples from the same paving contracts.....	51
Figure 4.3: Force-Displacement curves for sample C for various ligament lengths.....	53
Figure 4.4: Force-Displacement curves for sample D for various ligament lengths.....	54

Figure 4.5: Effective work of fracture of tank and recovered samples.....	55
Figure 4.6: Plastic work of failure for tank and recovered samples.....	56
Figure 4.7: Crack Tip Opening Displacement measurements for tank and recovered samples.....	57
Figure 4.8: Zinc content of tank and recovered samples in counts/second.....	60
Figure 4.9: Molybdenum content of tank and recovered samples in counts/second.....	61
Figure 4.10: Copper content of tank and recovered samples in counts/second.....	61
Figure 4.11: Calcium content of tank and recovered samples in counts/second.....	62
Figure 4.12: Sulphur content of tank and recovered samples in counts/second.....	63
Figure 4.13: Vanadium content of tank and recovered samples in counts/second.....	64
Figure: 4.14: Nickel content of tank and recovered samples in counts/second.....	64

Figure 4.15: High temperature grades of tank and recovered samples.....	65
Figure 4.16: Intermediate temperature grades of tank and recovered samples.....	66
Figure 4.17: Grade Span for tank and recovered samples.....	67
Figure 4.18: Black space diagram for contract J samples at different temperatures (a) and frequencies (b).....	69
Figure 4.19: Black space diagram for contract K samples at different temperatures (a) and frequencies (b).....	70
Figure 4.20: Black space diagram for contract L samples at different temperatures (a) and frequencies (b).....	71
Figure 4.21: Black space diagram for contract M samples at different temperatures (a) and frequencies (b).....	72

List of Tables

Table 4.1: XRF data for tank samples from 4 different paving contracts in Ontario recorded as peak heights in counts/second.....	59
Table 4.2: XRF data for recovered samples from 4 different paving contracts (8 separate locations) in Ontario recorded as peak heights in counts/second.....	59
Table 4.3: Stiffness values of the various contracts obtained from BBR testing.....	73

ABBREVIATIONS AND ACRONYMS

AASHTO	American Association of State and Highway Transportation Officials
BBR	Bending Beam Rheometer
CTOD	Crack Tip Opening Displacement
DENT	Double-Edge-Notched Tension
DSR	Dynamic Shear Rheometer
EBBR	Extended Bending Beam Rheometer
EWf	Essential Work of Fracture
LS	Laboratory Standard Test Method
m(t)	Slope of the Creep Stiffness Master Curve (m-value)
S(t)	Time-dependent Flexural Creep Stiffness, MPa
MPa	Mega Pascal
PG	Performance Grade
PAV	Pressure Aging Vessel
HMA	Hot Mix Asphalt
RTFO	Rolling Thin Film Oven
SHRP	Strategic Highway Research Program
SUPERPAVE™	SUperior PERforming Asphalt PAVement
TFOT	Thin Film Oven Test

CHAPTER 1

INTRODUCTION

1.1 Overview

The word asphalt is derived from the Greek word “asphaltic” which means to make firm or stable. The material has been in use since the dawn of civilization and is known as man’s oldest engineering material [1]. Its application as cement for bonding, coating and waterproofing has been exploited from past to present and surely is one of the most versatile products in nature [1].

The main constituents of asphalt are bitumen and it is either found in nature or obtained as a product of petroleum processing [2]. Natural asphalt deposits such as Trinidad lake asphalt, “tar sands” found mostly in western Canada and the Le Brea “tar” pits near Los Angeles were used by ancient Babylonians, Greeks, Egyptians and Romans as road building and waterproofing material [1,2]. Other sources of natural asphalt include porous rocks such as limestone (rock asphalt) [2]. Rock asphalt was first used in sidewalk surfacing around 1802 in France and then 1838 in Philadelphia. However, the first asphalt pavement was constructed in Newark, New Jersey in 1870 while the first sheet asphalt (fine sand mix) pavement was constructed in Washington D.C. six years later using imported lake asphalt.

In the early 1900’s, it was discovered that asphalt could be produced by refining crude petroleum, this discovery led to a widespread expansion of the asphalt paving industry in the United States. Though asphalt has many other applications about 85 percent of asphalt produced from crude oil refining is used for road construction. These days nearly all asphalt used are sourced from crude oil refining. The rapid growth in asphalt usage is shown in Figure 1.1 below [1,2].

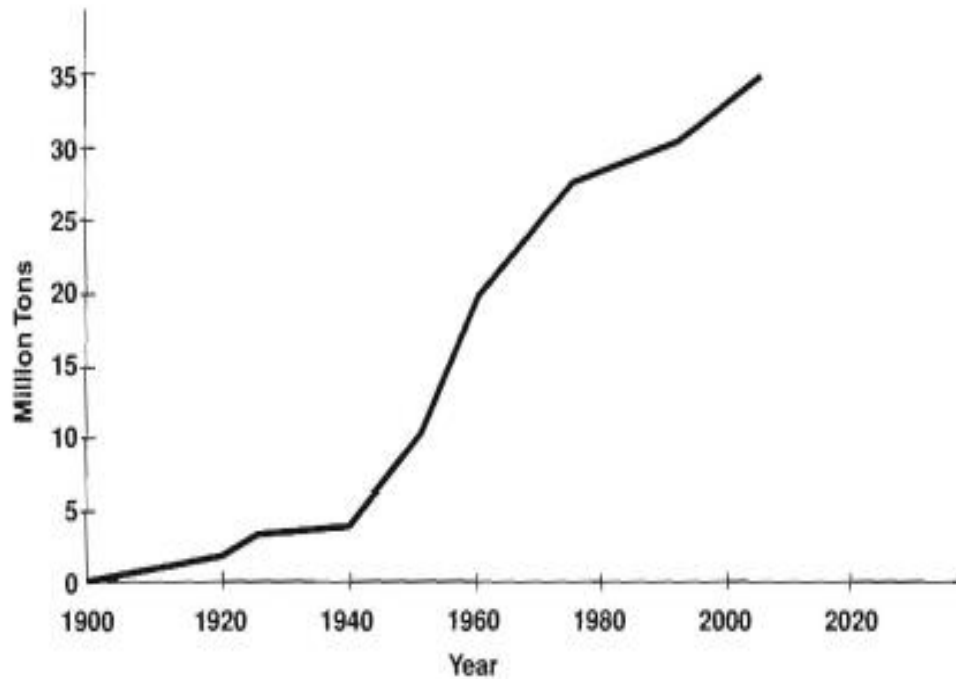


Figure 1.1: Annual asphalt usage in the U.S. [2].

With this growth in the asphalt industry, people became interested in determining the physical properties and behaviour of asphalt (mainly to ensure the durability of asphalt roads). A number of tests and procedures were developed in the early 1900s including possibly the first scientific approach to designing asphalt paving mixes (determination of asphalt content based on air voids) [1].

1.2 Composition of Asphalt

Asphalt is a complex mixture obtained from crude petroleum which is basically organic matter subjected to varying condition of temperature and pressure for millions of years [2]. From generic elemental analysis, asphalt was found to be made up of approximately 84 percent carbon,

1 percent oxygen, 10 percent hydrogen, and the remaining constituents being trace amounts of vanadium, sulfur, nitrogen, nickel and iron [3]. These trace elements often replace carbon atoms in the asphalt molecule and are responsible for many of asphalt's unique chemical and physical properties due to the molecular interactions they cause. For example, sulfur reacts more readily to incorporate oxygen (oxidation) in the asphalt molecular structure than carbon and hydrogen [2]. "Oxidation is the primary part of the overall asphalt aging process" [2]. Also, these trace elements can give some idea about the crude source of the asphalt binder [2].

1.3 Separation of Components

Separation of asphalt components can be done by using the differences in solubility of the various components in different solvents. The two methods that are usually used are the Corbett (chromatographic) method and the Rostler (precipitation) method. These methods however do not give discreet chemical species but rather complex species with varying properties which leads to difficulty in predicting asphalt behaviour.

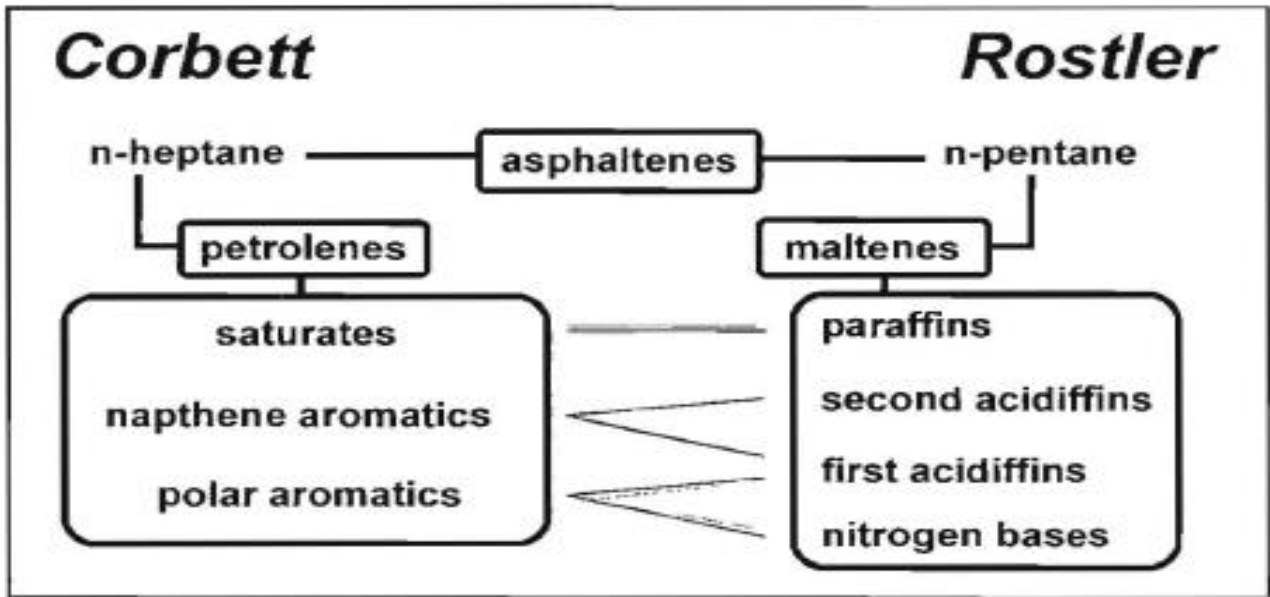


Figure 1.2: Asphalt cement component [2].

1.4 Asphalt Behaviour

Asphalt is a viscoelastic material whose elastic and viscous behaviour depends on factors such as temperature and time of loading [4]. It behaves like an elastic solid at low temperature whereas at high temperature it exhibits viscous behaviour, in between these two extremes (i.e., intermediate temperatures) asphalt exhibits both elastic and viscous behaviour [5]. Asphalt behaviour can be studied based on the following parameters:

- High temperature behaviour
- Low temperature behaviour
- Intermediate temperature behaviour
- Aging behaviour

1.4.1 High Temperature Behaviour

Since asphalt exhibits viscous behaviour at high temperature it makes sense to briefly discuss viscosity. It is important to consider the effects of temperature on viscosity mainly because asphalt is subjected to huge temperature variations [6]. Viscosity is simply a measure of the internal friction of a liquid and this becomes more observable when layers of the liquid move relative to each other [5].

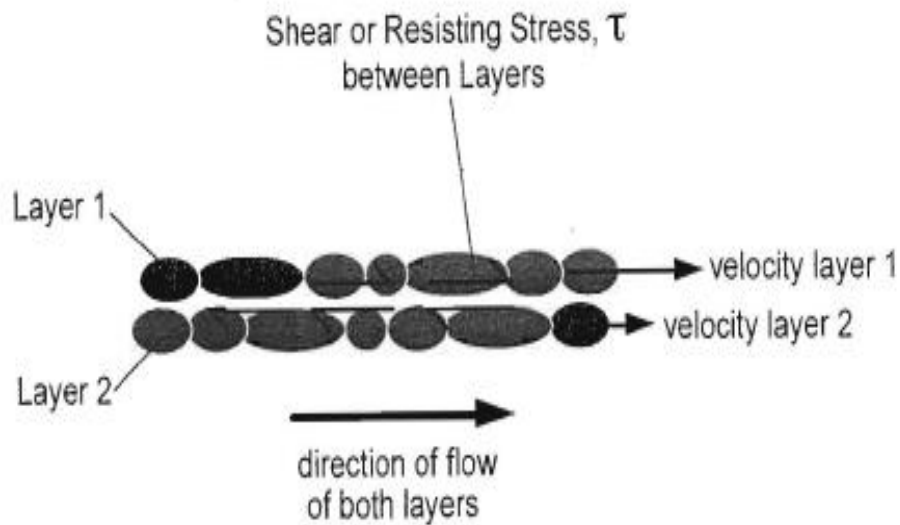


Figure 1.3: Microscopic shot of liquid flow [2].

The figure above shows how liquid layers move relative to each when viewed under a powerful microscope. Shear or resisting stress indicated in Figure 1.3 occurs whenever a liquid is sprayed, poured, mixed or spread and is the force required to cause movement of the liquid opposed to friction. In other words, the greater the friction (more viscous), the greater the force required to cause movement (shear) [5].

Depending on the type/content of an asphalt binder, it may behave as either a Newtonian or non-Newtonian fluid at high temperature [2].

1.4.1.1 Newtonian Fluid Behaviour

Typically, unmodified asphalt binders exhibit this type of behaviour at high temperature [7].

These fluids show a linear relationship between shear stress and rate of shear strain and viscosity remains constant at a given temperature regardless of the shear rate [2,5].

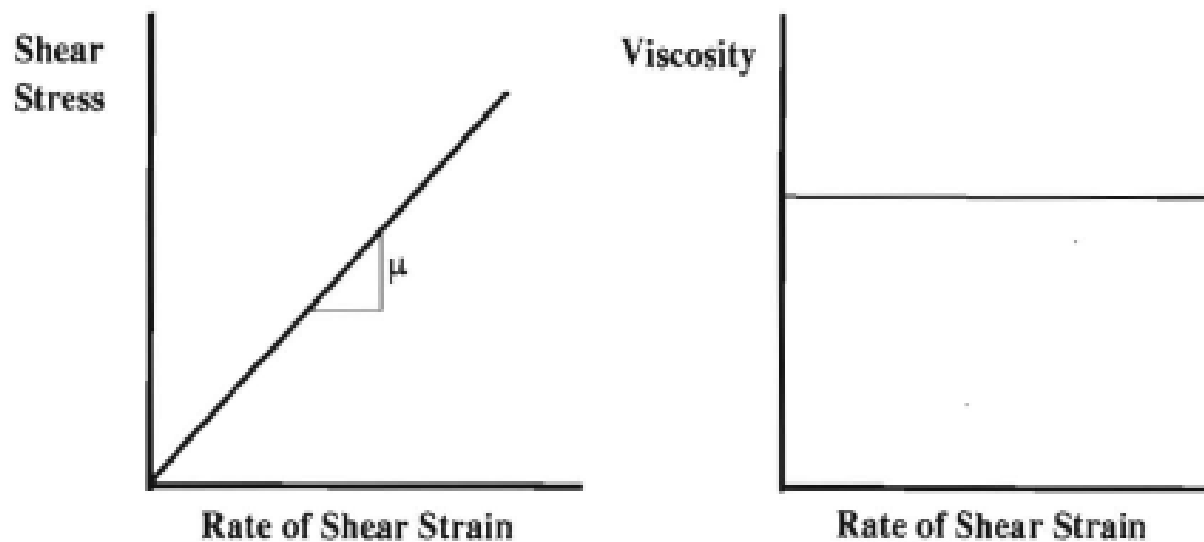


Figure 1.4: Newtonian fluid behaviour [2].

1.4.1.2 Non-Newtonian Fluid Behaviour

On the other hand, modified asphalt binders exhibit non-Newtonian behaviour and this could be either of two types of non-Newtonian behaviour (pseudo-plastic or dilatant flow behaviours) [2,5].

For pseudo-plastic flow behaviour (also referred to as shear thinning) [7], viscosity decreases as shear rate is increased. This basically means the faster the fluid is stirred, the thinner it becomes [2,5].

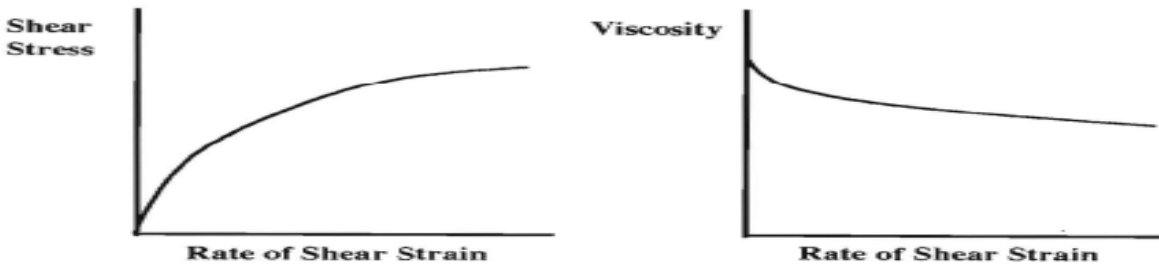


Figure 1.5: Pseudo-plastic flow behaviour [2].

Alternatively, for dilatant flow behaviour (also known as shear thickening) [7], viscosity increases as shear rate increases, which means the faster the fluid is stirred the thicker it becomes [2,5].

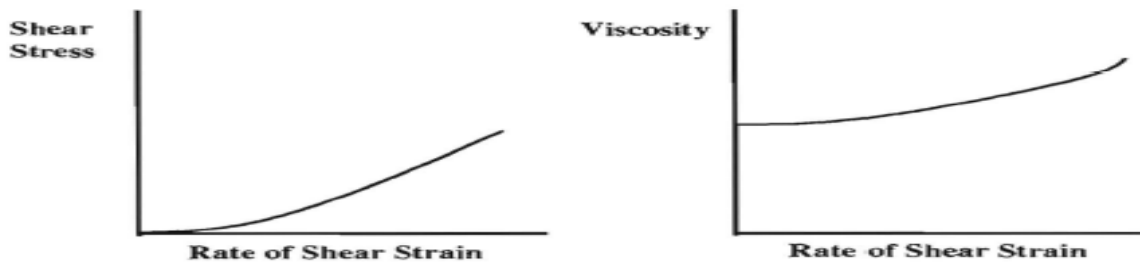


Figure 1.6: Dilatant Flow Behaviour [2].

1.4.2 Low Temperature Behaviour

At low temperature, asphalt cement behaves like an elastic solid. It deforms when a load is applied on it and returns to its original state when the load is taken off, just like a rubber band. However just like the rubber band, when excessive load is applied it becomes brittle and breaks. For asphalt cement at low temperature, this excessive load is equivalent to internal stresses that build up within the asphalt cement structure when it tries to shrink while being restrained by lower layers in the pavement. This phenomenon is known as thermal temperature cracking [2] and will be looked at extensively in the next chapter.

1.4.3 Intermediate Temperature Behaviour

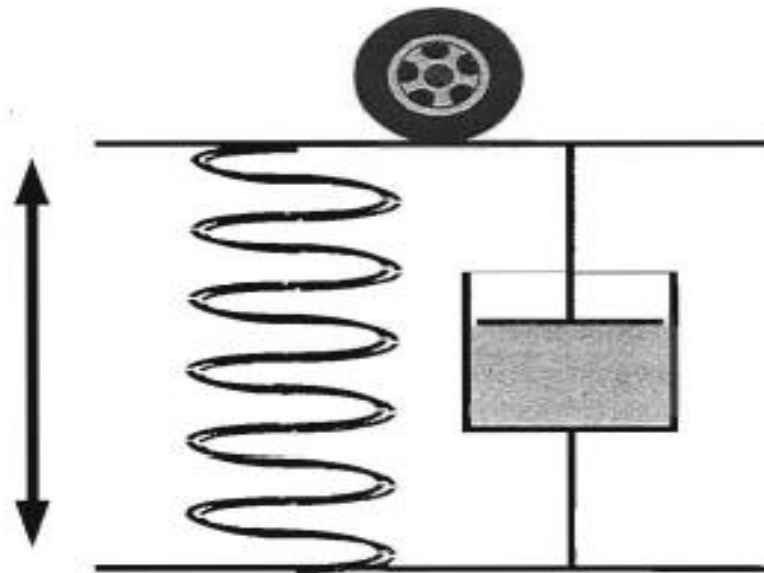


Figure 1.7: "Spring-Dashpot" model [2].

Asphalt at intermediate temperature exhibits viscoelastic characteristics depending of the rate of loading as well as temperature. This is best illustrated by Figure 1.7 above. When force is applied to the asphalt, a parallel reaction occurs in both the spring and the dashpot. The spring represents the elastic reaction while the dashpot represents the viscous reaction.

Asphalt at intermediate temperature exhibits viscoelastic characteristics depending of the rate of loading as well as temperature. This is best illustrated by Figure 1.7 above. When force is applied to the asphalt, a parallel reaction occurs in both the spring and the dashpot. The spring represents the elastic reaction while the dashpot represents the viscous reaction [2].

1.4.4 Aging Behaviour

Aging behaviour is observed when asphalt cement reacts with diffused oxygen from the atmosphere causing a change in the composition and structure of the bitumen hydrocarbons in the asphalt mixture and thereby leading to an irreversible process called oxidative or age hardening which in turn leads to an overall reduction in the pavement durability [2,8]. According to Allen et al., the bitumen component represents a very important component in the asphalt pavement and thus controls the overall performance of the asphalt pavement. Oxidative hardening occurs at a relatively slow rate except during warm conditions or climate where it occurs at a faster rate. This means that the older a pavement is, the more susceptible it is to cracking [2], due to the overall pavement/asphalt mixture stiffness this phenomenon causes [8]. Cases also exist where due to improper compaction of asphalt pavements premature aging occurs due to interconnected air voids that may form within the pavement [2]. Oxidative hardening has

an upside though; in that it leads to increased rutting resistance. However, it also accelerates fatigue, low temperature cracking and moisture damage [8].

1.5 Objectives and Scope

This research covers thermal cracking and physical hardening phenomenon by comparing results from testing asphalt binder samples obtained from the 'tank' prior to paving (tank samples) and recovered samples for the same contracts with aim of explaining why asphalt binders that have passed quality assurance tests fail prematurely.

The study will also attempt to find out if the short testing time and automated procedure of the torsion experiments can replace the already established, longer testing and tedious procedure of the EBBR.

CHAPTER 2

BACKGROUND

2.1 Asphalt Distresses

Generally due to its durability and resilience asphalt cement is recommended for many road construction applications. However, despite the high durability of this material it is still susceptible to elements such as rain, sunlight, oxygen, chemicals, thermal stresses and constant traffic loading and hence can deteriorate over time.

The lifespan of asphalt pavements can be shortened either through poor construction techniques or exposure to extreme environmental conditions for a long period of time [10].

Poor construction techniques include [11]:

- Over/under compacting asphalt pavement
- Improper compacting of the base below the asphalt pavement
- Spreading or pouring asphalt binders at wrong temperatures (especially if the temperature is not high enough); and
- Poor drainage.

The type of distresses that asphalt pavements can undergo are [12]:

- Fatigue cracking;
- Moisture damage;
- Rutting; and
- Thermal (low temperature) cracking.

2.1.1 Fatigue Cracking

Smith [13] defined fatigue cracking as the phenomenon of fracture after a material has been subjected to repeated or fluctuating stress with a maximum value less than the tensile strength of the material. This usually happens when the pavement is exposed to heavy or repetitive loads which leads to stress that is more than the fatigue limit of the pavement, which in turn leads to fracture [10].

Pavements can undergo fatigue cracking prematurely when underlying layers of the pavement become weakened by excessive moisture or high traffic of overweight trucks if the right pavement thickness is not ensured during construction [14]. For thicker pavements fatigue cracking occurs from surface to bottom layers while for thinner pavements fatigue cracking occurs from the bottom to the surface. This is due to high tensile strains on the surface and bottom respectively [10].

Fatigue cracking occurs in three stages [13]:

- Crack Initiation - This is when micro cracks begin to form.
- Crack Propagation – Here micro cracks develop into macro cracks with stable crack growth.
- Disintegration – At this stage, complete loss of fatigue life occurs. There is collapse and complete failure of the pavement due to unstable crack growth.

The dynamic shear rheometer (DSR) can be used to predict the fatigue behaviour of asphalt binders by measuring the fatigue resistance factor, which is $G^* \sin \delta$, where G^* is the complex modulus and δ represents the phase angle.



Figure 2.1: Fatigue (alligator) cracking [15].

2.1.2 Moisture Damage

Moisture damage occurs when asphalt cement is stripped from the aggregate due to water penetration as a result of rain, snow and absorption of ground water into the structure of the pavement. Moisture affects pavement structure in the following ways [14]:

- Weakening or breaking bonds between asphalt binder and aggregate.
- Freezing individual aggregates.

Using highly viscous asphalt binders increase adhesiveness and reduce the interference of water with the bonding. However, carboxylic acids and sulfoxides that exist in asphalts can be easily displaced by water molecules, increasing sensitivity to moisture.

Aggregate composition, size and number of pores also affect moisture absorption [14].

Moisture damage can be controlled by proper compaction and drainage, and the use of anti-stripping agents [12].



Figure 2.2: Moisture damage (stripping) [16].

2.1.3 Rutting

Rutting is a pavement distress that occurs at high temperatures. At high temperature asphalt binders become less viscous which leads to formation of ruts or tracks on the surface of pavements due to easy flow of the binder under heavy traffic loads [10].

Moisture and air penetration can also weaken the sublayer of the pavement resulting in rutting [17,18].

The rutting resistance factor, $G^*/\sin \delta$ is used to predict rutting and is measured using the DSR [19].



Figure 2.3: Rutting [20].

2.1.4 Thermal Cracking

Thermal cracking is a phenomenon that usually occurs in cold regions (low temperature cracking) and also in areas where large temperature extremes occur on a daily basis. Thermal stresses that occur during cooling are usually responsible for low temperature cracking of asphalt pavements. It has been observed that if the stress is equal to or greater than the tensile strength of the asphalt, it may lead to the appearance of surface micro-cracks which after subsequent low

temperature cycles will spread deeper into the pavement. The cracking process consequently leads to poor ride quality, short service life and high maintenance costs [19].

Several origins exist when considering the source of thermal stresses, these include bending stresses which results from thermal or stiffness gradients with depth, or tensile stresses within the binder itself caused by cooling when thermal expansion coefficients between asphalt and aggregate differ [21].



Figure 2.4: Thermal cracking of asphalt pavement [22,23].

2.1.4.1 Factors Resulting in Thermal Cracking

Factors that lead to low temperature cracking are [19]:

- Environmental factors;
- Pavement structure; and
- Binder consistency (material factors).

2.1.4.1.1 Environmental Factors

Major environmental factors that affect asphalt pavements and lead to thermal cracking are temperature, cooling rate and pavement age [25].

When the exposed surface layer of the pavement encounters low temperature below its glass transition temperature for a long time, micro cracks begin to form. This is usually because of accumulation of stresses in the pavement due to resistance to contraction within the pavement layers as friction increases [10,26].

Cooling rate is another major environmental factor responsible for thermal cracking and determines the rate at which cracks form as well as the magnitude. The faster a pavement cools the more susceptible it is to thermal cracking [26].

Due to the increase in binder stiffness as the pavement becomes older, the pavement becomes increasingly susceptible to thermal cracking. Aging affects the asphalt binder's ability to relax stresses [27].

2.1.4.1.2 Pavement Structure

The structure of the asphalt pavement also determines its susceptibility to thermal cracking. For example, thicker pavements are less susceptible to thermal cracking compared to thinner pavements and narrow pavements most often have closer thermal cracks than those of wide pavements [26].

Also, the friction coefficient between the base course and asphalt concrete layer can contribute to thermal cracking. Usually, the base course has a lower thermal coefficient of contraction and

when it is perfectly bonded to the asphalt concrete layer, it reduces the thermal coefficient of the asphalt concrete layer as well [25,26].

Construction defects that occur during high temperature compaction of asphalt layers and pavement cooling also leave pavements vulnerable to thermal cracking.

2.1.4.1.3 Binder Consistency (Material Factors)

Binder consistency is one of the most important factors that affect the low temperature behaviour of asphalt pavements [19]. It is important to consider the type of asphalt binder used in pavement construction due to the wide variety of viscoelastic properties of the different types of asphalt available.

The stiffness-temperature relationship is an important factor which determines the extent of thermal cracking in asphalt pavements [26]. Binder stiffness gives a fairly good idea about how a pavement will perform in extremely low temperature conditions [25].

The following binder consistency parameters have a strong influence in low temperature cracking in asphalt pavements:

- Stiffness
- Viscosity
- Penetration
- Softening point

Tests used to determine the extent of these parameters will be looked at later on in this chapter.

For the purpose of this research, more emphasis is going to be placed on binder consistency.

2.2 Asphalt Binder Testing Procedures

- Conventional Test Procedures
- SuperPave Specification Procedures
- Newly Approved Test Procedures (Accepted by MTO and recently by AASHTO)

2.2.1 Conventional Test Procedures

These methods were used for asphalt binder testing during the early 1900s and comprise of [28,29]:

- Penetration Tests
- Softening Point Tests
- Viscosity Tests

These tests however, are not performance related and hence give only empirical results [30]. The properties of asphalt binders were evaluated using four conventional grades namely: Cutback, Oxidized, Hard and Penetration grades. The penetration grade which is obtained from the use of the needle penetration method is considered the most important among the grades in terms of pavement construction [10,25,31].

The Oxidized and Hard grades are determined through a combination of the viscosity and softening point methods while the just viscosity test is used to determine the Cutback grade [10,30].

2.2.1.1 Penetration Tests

The penetration test was developed in 1888 by H.C. Bowen of the Barber Asphalt Paving Company [32]. In this test, the consistency of an asphalt binder with a load of 100g is measured at 25⁰C for 5 seconds. The test method is used to classify rather than measure the performance of the asphalt binder. The load is essentially a needle which penetrates the surface of the asphalt binder [33]. The depth of penetration is measured in decimillimeters (0.1mm). The relationship between the asphalt binder hardness and temperature are analyzed using the following equation [34]:

$\log P = AT + K$, where

P = Penetration

T =Temperature

K = Constant

A = Temperature Susceptibility/Performance Index

$$A = [\log (T_{1PEN}) - \log (T_{2PEN})]/T_1 - T_2$$

T_{1PEN} and T_{2PEN} represent penetration at T_1 and T_2 respectively.



Figure 2.5: Penetration test equipment [35].

2.2.1.2 Softening Point Tests

These tests are used to determine the flow of asphalt binders at elevated/in-service temperatures.

Here, the test is carried out using a ring and ball apparatus immersed in distilled water or ethylene glycol at temperatures between 30⁰C - 157⁰C. The softening point is measured at the

temperature at which the asphalt binder can no longer resist the push of the ball in the ring shown in the apparatus below [36].

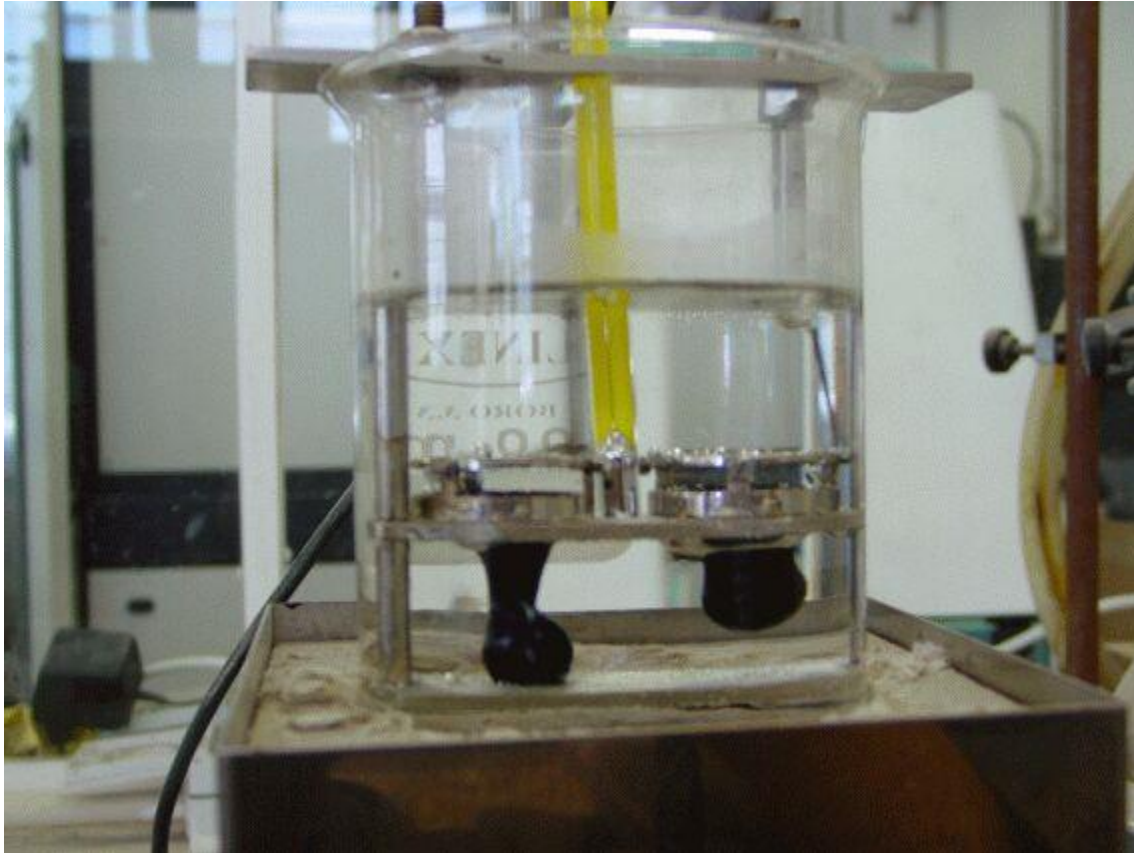


Figure 2.6: Ring and ball apparatus [37].

2.2.1.3 Viscosity Tests

These tests are performed on either unaged or RTFO-aged asphalt binders. The unaged (AC grading) asphalt binders represent the binder before HMA manufacturing while RTFO-aged (AR grading) asphalt binders are characteristic of the binder after HMA manufacturing.

The test basically measures the internal friction of the asphalt binder as its layers slide past each other [5] and was developed in an effort to improve upon the Penetration Test [32].



Figure 2.7: Viscosity test apparatus [38].

2.2.2 Superpave Specification Procedures

Due to the empirical nature of results obtained from the conventional method, in the late 1980s the Strategic Highway Research Program (SHRP) began working on tests that measure the physical properties of asphalt. After 50 million dollars' worth of research, the SHRP came up with the Superpave binder specification. The Superpave test were a good improvement on the conventional test methods as they could measure physical properties directly related to field performance by engineering principles and simulate in-service pavement conditions [2]. The advent of the Superpave specification tests gave hope of being able to achieve the aim of reducing the various forms of pavement distresses [10]. An important feature of the Superpave specification is that the specified physical property being measured remains constant but the temperature at which the measurement is being done changes for different grades of asphalt [2]. These grades were assigned as Performance Grade (PG) or Performance Grade Asphalt Cement (PGAC) XX-YY where XX represents the maximum working limits of the asphalt binder while YY represents the minimum working limit [31].

Asphalt binders age when they are exposed to oxygen and through volatilization of organic components of the binder during/after hot mixing and construction. Before asphalt binders undergo the Superpave physical tests, these conditions are simulated using the following [2]:

- Rolling Thin Film Oven (RTFO)
- Pressure Aging Vessel (PAV)

2.2.2.1 Rolling Thin Film Oven (RTFO)

The RTFO is used to simulate the aging that occurs during hot mixing and construction due to high temperature and air flow involved in these processes. It also gives a measure of volatile organic compounds lost during these processes [2].

The RTFO is an electrically-heated convection oven that contains a circular sample carriage that holds the sample bottles and rotates about its center [2]. An air jet in the oven blows air into the thin film of asphalt binder as it rotates on the sample carriage. The binder in the sample bottles weigh about 35 grams and is heated in the oven for 85 minutes at 163°C.



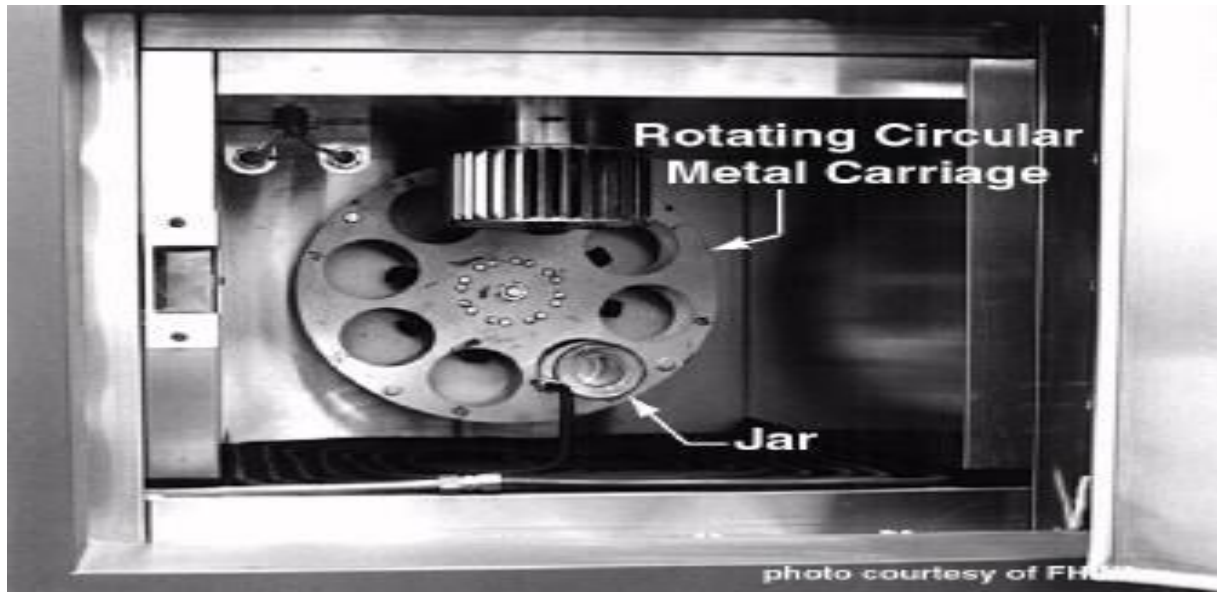


Figure 2.8: Rolling Thin Film Oven [39,40].

After the asphalt binder has been aged in the RTFO, some of it undergoes physical tests in the DSR and the rest is further aged in a PAV [2,31].

2.2.2.2 Pressure Aging Vessel (PAV)

The PAV is used to simulate aging that occurs after the asphalt pavement has been constructed (long term aging). The binder to be PAV aged should have already been RTFO aged to give a good representation of asphalt binder that has undergone hot mixing and placement [2]. The samples to be tested are poured in PAV pans on a rack and placed in the PAV. The sample is then subjected to temperatures between 95 to 110°C depending on the field conditions and left for 20 hours at a pressure of 2080 kPa [41].



Figure 2.9: Pressure Aging Vessel and its components [42].

After the above aging procedures have been carried out, the next step is carrying out the Superpave specification tests:

- Bending Beam Rheometer (BBR) Test
- Dynamic Shear Rheometer (DSR) Test

2.2.2.3 Bending Beam Rheometer (BBR) Test

The BBR measures how much of an asphalt binder creeps or deflects when a constant load is applied to it at constant temperature [2]. The temperatures at which the BBR tests are carried out are low temperatures since this test is designed to simulate the lowest in-service temperatures of asphalt pavements.

This testing method was developed by the Strategic High Research Program (SHRP) in an effort to address thermal cracking [28,41] and was later accepted in AASHTO M320 standard protocol as specification criteria for passing or failing asphalt binders [43]. The AASHTO M320 specification was based on research done in Amsterdam by Shell laboratories in the 1950s and 1960s. From this research, they concluded that the failure properties of the asphalt pavement are strongly related to the stiffness of the asphalt binder used at a constant loading time. To perform the BBR tests, the asphalt binder is moulded into beams and conditioned in solvent bath filled with solvent that will not freeze at the low temperatures at which the binder will be conditioned. Solvents used are usually ethanol, methanol, ethylene glycol or mixtures of these. Also, testing and conditioning temperatures are the same in this test [2].

The beams are conditioned for one hour at the test temperature, which is normally 10°C above the designed pavement temperature and this is based on the superposition principle to reduce the

test time from 2 hours to 60 seconds [41,44]. The beam is loaded on a “three-point bend” setup and the BBR measures Creep Stiffness, $S(t)$ and the slope of the creep stiffness master curve of the binder known as the m-value at 60 seconds. To obtain the master curve, the stiffness of the beam is measured at loading times of 8, 15, 30, 60, 120 and 240 seconds [2]. The m-value and $S(t)$ are related to the performance of the asphalt pavement at low temperatures [10]. The m-value is a measure of the asphalt binder’s ability to relax stresses [43].

If the m-value is equal to or greater than 0.3 and has creep stiffness with a maximum value of 300MPa, then the sample is said to have passed the specification. This implies the asphalt binder can relax stresses faster and hence has decreased thermal stress leading to decreased thermal cracking [45].

Creep stiffness is given by the equation [2]:

$$S(t) = PL^3/4bh^3\delta(t)$$

Where, $S(t)$ = Creep stiffness(MPA) at time, t

P = applied constant load, N

L = distance between beam supports, 102mm

b = beam width, 12.5mm

h = beam thickness, 6.25mm

$\delta(t)$ = deflection (mm) at time t.

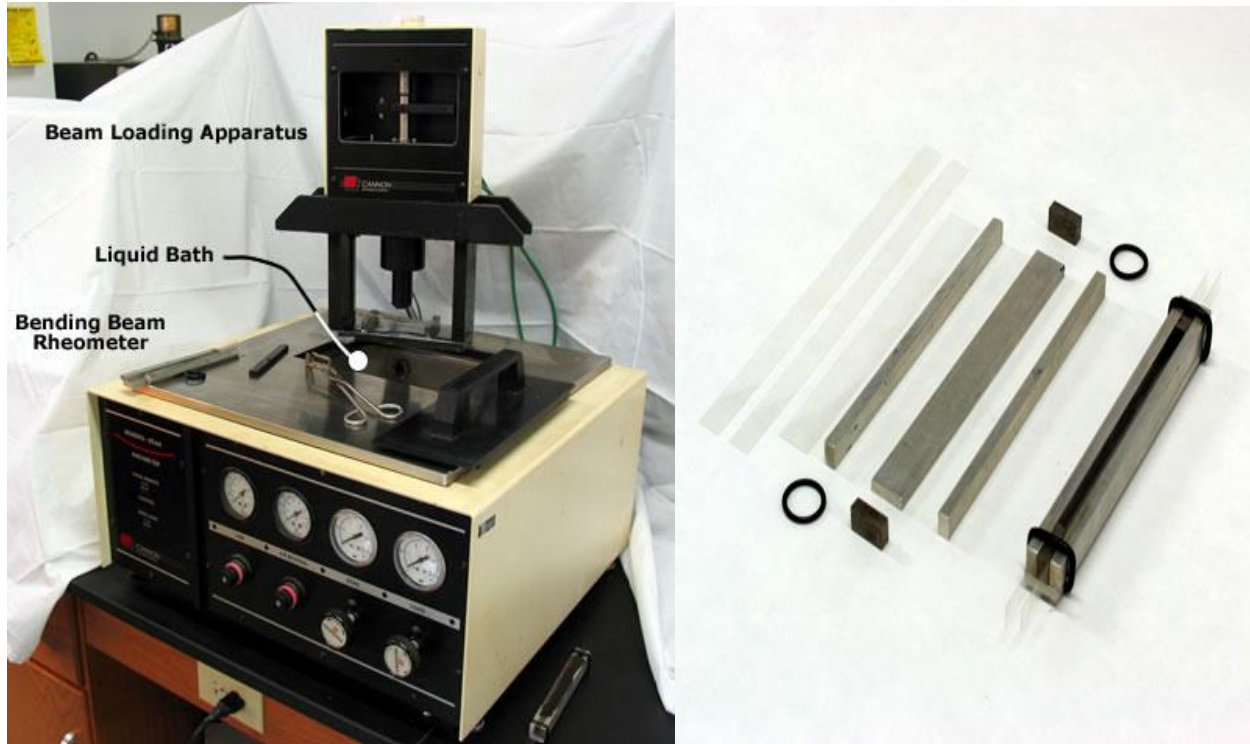


Figure 2.10: Bending Beam Rheometer [46].

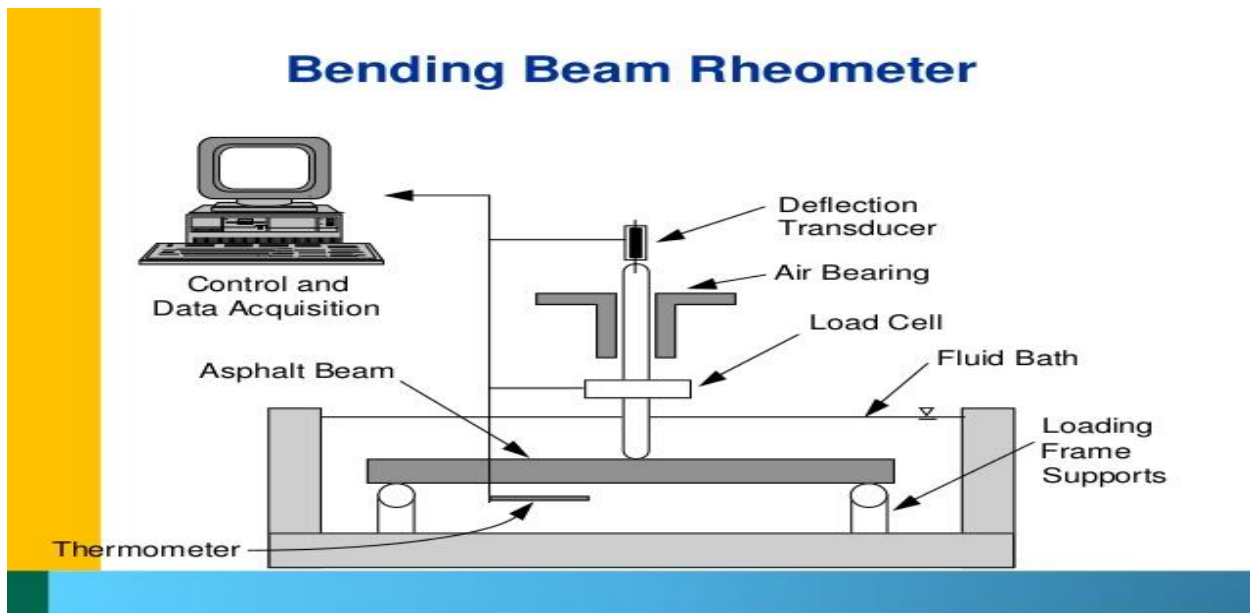


Figure 2.11: Schematic diagram of the BBR [47].

2.2.2.4 Dynamic Shear Rheometer (DSR) Test

The DSR is used to measure the rheological properties (complex shear modulus and phase angle) of asphalt binders at intermediate to high temperatures. The DSR is used for asphalt binder testing because it incorporates two important factors that affect asphalt behaviour; loading time and temperature. The complex shear modulus and phase angle measured in the DSR represent the measure of the total resistance of the asphalt binder to deformation and relative amount of recoverable and non-recoverable deformation respectively [48].

The elastic component, G' and viscous component, G'' of unaged, RTFO-aged and PAV-aged asphalt binders are also measured to determine the high and intermediate temperature grade of the binder. These two components are associated with thermal cracking at low temperatures (for G') and rutting at high temperatures (for G'') [2].

The complex shear modulus is given by [45]:

$$G^* = \tau_o / \gamma_o$$

τ_o = peak shear stress

γ_o = peak shear strain

From the peak shear stress and strain, we obtain shear stress (τ) and oscillatory strain (γ) respectively [45]:

$$\tau = \tau_o \sin(\omega t + \delta)$$

$$\gamma = \gamma_o \sin \omega t$$

δ = phase angle

ω = angular velocity in radians /second

t = time.

From AASHTO specification, the relation $G^*/\sin\delta$ gives the high temperature performance grade of the asphalt binder and should be greater than 1.00kPa for unaged samples but greater than 2.20kPa for RTFO-aged samples. This is done to investigate rutting behaviour.

$G^*\sin\delta$ gives the intermediate temperature performance grade. Here PAV-aged samples are used and $G^*\sin\delta$ should not exceed 5000kPa. This is used for fatigue cracking investigation [2].



Figure 2.12: AR 2000 Dynamic Shear Rheometer [49].

2.2.3 Newly Approved Test Procedures (Accepted by MTO and recently by AASHTO)

The need to come up with these new procedures arose from the fact that the AASHTO M320 specification did not take into account physical aging/hardening when measuring rheological properties. This meant that the tests being carried out on asphalt binders was not a true a representation of in-service conditions since physical hardening has been proven to occur during the service life of asphalt pavements [50-53].

In view of this, the Ministry of Transportation Ontario (MTO) collaborated with Queen's University and developed the following test procedures which have now been accepted as part AASHTO specification [54]:

- Extended Bending Beam Rheometer (EBBR) test (LS-308) [55]
- Double-Edge-Notched Tension (DENT) test (LS-299) [56]
- Modified Pressure Aging Vessel protocols (LS-228) [57]

2.2.3.1 Extended Bending Beam Rheometer (EBBR) Test (LS-308)

The regular BBR tests were not sufficient in simulating in-service condition because samples were conditioned for only an hour and this meant that there was not enough time for physical hardening to be considered. Therefore, there was a need for the development of the EBBR, which conditions asphalt binder samples for 1 hour, then 24 and 72 hours. This efficiently accounts for the physical hardening effect and thermal cracking in pavements [52].

In the EBBR tests, two conditioning temperatures are considered, which are:

- $T_1 = T_{\text{design}} + 10^\circ\text{C}$ and
- $T_2 = T_{\text{design}} + 20^\circ\text{C}$.

where T_{design} is, the lowest temperature designed for the pavement, prior to testing.

Just as employed in the regular BBR, the AASHTO M320 is used to determine the exact grade of the asphalt binder by using a pass and a fail temperature value through interpolation. The grade temperature and subsequent grade loss can be evaluated after a particular temperature conditioning period. The best grade lost can be evaluated by taking the difference between the least warm and least cold limiting temperature (where S (60s) reaches 300 MPa and m (60s) reaches 0.3) [18, 25]. The worst grade on the other hand can be evaluated by taking the difference of the warmest and coldest limiting temperature (where S (60s) reaches 300 MPa and m (60s) reaches 0.3) [18, 25].

This test procedure has proven thus far as effective way of evaluating thermal cracking in asphalt binders [29].

2.2.3.2 Double-Edge-Notched Tension (DENT) Test (LS-299)

The DENT test is used to evaluate the ductile and brittle properties of asphalt binders. It is based on work done by Cotterell and Reddel on the theory of essential work of fracture [58]. The double edge notched tension test measures the essential work of failure in asphalt binders, the plastic work of failure and the critical crack tip opening displacement (CTOD) [56]. This test is

carried out by pouring hot asphalt binder into special molds to form notched specimens with the distance between the opposite notches ranging as 5 mm, 10 mm and 15 mm. The specimens are conditioned in a water bath at a specified temperature. After conditioning, the test is then carried out by stretching the specimens until failure as shown below [25].

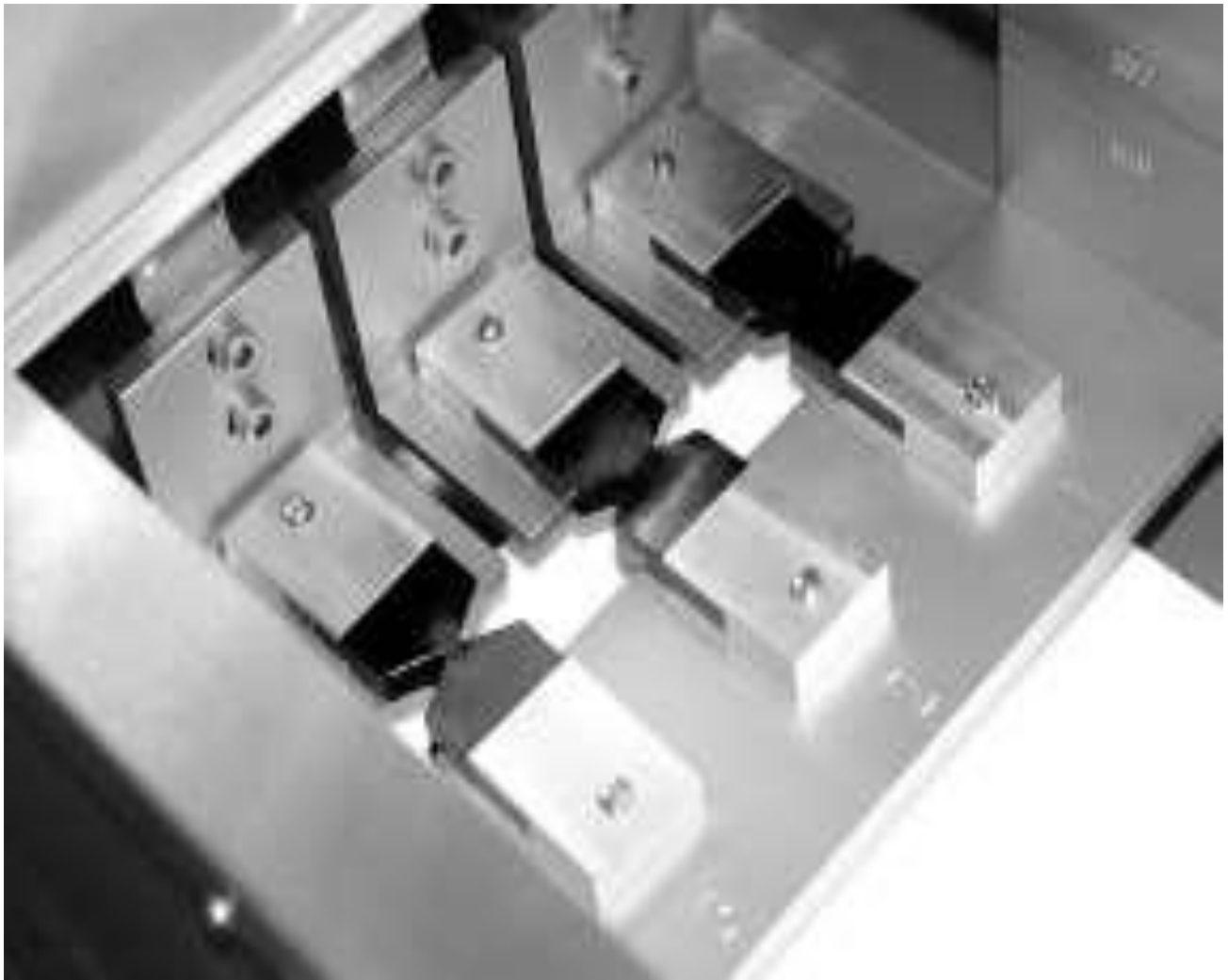


Figure 2.13: Double Edged-Notched Tension (DENT) test [59].

The total work of fracture is the sum of the essential work of fracture energy and the plastic work of fracture energy. The total work fracture (W_t) is evaluated from the total area under the force-displacement curve per the equation:

$$W_t = W_e + W_p$$

Where, W_e = essential work of failure

W_p = plastic work of failure

$$W_e = w_e \times LB$$

$$W_p = w_p \times \beta L^2 B$$

Where, w_e = specific essential work of fracture (J/ m^2)

w_p = specific plastic work of fracture (J/ m^2)

L = the ligament length in the DENT specimen (m)

B = the thickness of the sample (m)

β = the shape factor of the plastic zone, which is dependent on the geometry.

A plot of the specific total work of failure, w_t , against the ligament length, L , gives a straight line with slope and intercept on the w_t axis [25].

The fatigue cracking resistance of an asphalt binder is predicted by CTOD, and this is given by the equation [60]:

$$\delta_t = w_f / \sigma n$$

Where, δ_t = crack tip opening displacement parameter (m)

σ_n = net section stress or yield stress (N/m^2), determined from the 5mm ligament length of the DENT mold [25].

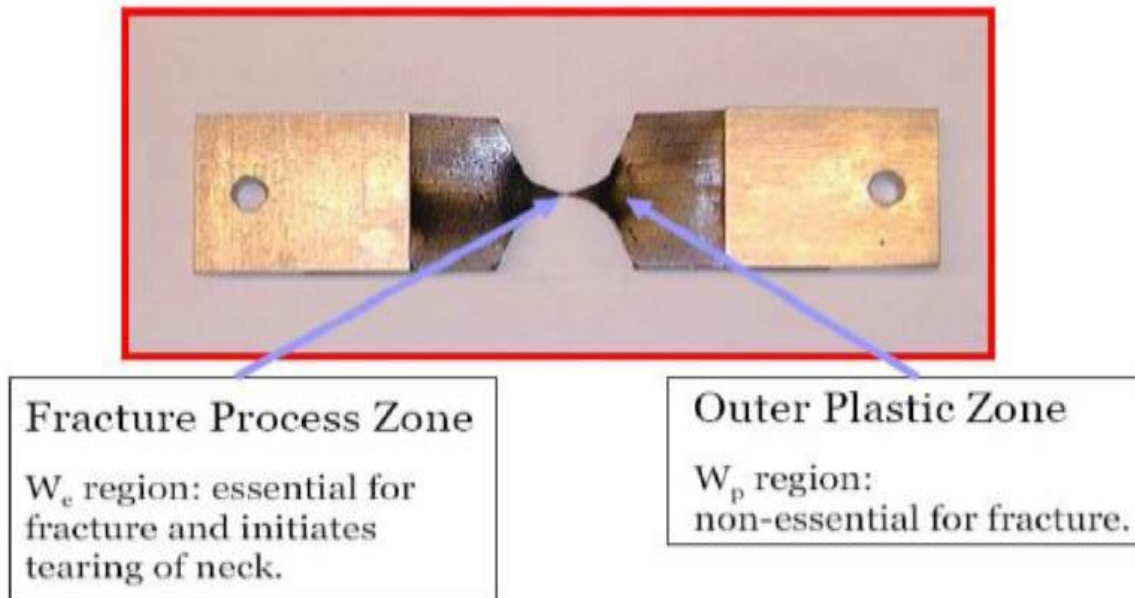


Figure 2.14: Fracture process zone and outer plastic zone of asphalt binder [61].

2.2.3.3 Modified Pressure Aging Vessel protocols (LS-228)

It was found out that the existing PAV method did not efficiently facilitate the prediction of fatigue and thermal cracking distress, hence the modified PAV protocols [62-64]. This test is carried out in two ways. In the first method, the weight of the asphalt sample is reduced from 50 +/- 0.5 grams to 12.5 +/- 0.5 grams. This means the thickness of the film decreases from 3.2 mm to approximately 0.8 mm. To simulate a moist environment, one empty TFOT stainless steel pan is loaded with 50 grams of distilled water [31]. The second method involves increasing the duration of aging is increased from 20 hours to 40 hours. One empty TFOT stainless steel pan is

loaded with 50 grams of distilled water to once again simulate the presence of moisture but here the standard film thickness is maintained [57].

This improved method is efficient in exposing lesser quality asphalts due to the presence of moisture and exposure of the thinner films for longer times during aging [65].

CHAPTER 3

MATERIALS & EXPERIMENTAL METHODS

3.1 Materials

Asphalt binders that were used in this research were those obtained from the tank prior to construction of the asphalt pavement (tank samples) and those recovered from already constructed pavements (recovered samples). These samples were for road construction done on Highways, 7, 11, 12, 17, 61, 108, 416 and 417, representing the North Eastern, Eastern and Central regions.

3.1.1 Asphalt Cement Aging

The tank samples were made to undergo both short-term and long-term aging of asphalt binders. Short-term aging which occurs during hot-mixing was simulated by the Rolling Thin Film Oven (RTFO) test while long-term aging which occurs after hot-mixing and pavement construction simulated using the Pressure Aging Vessel (PAV) test [31].

3.1.2 Rolling Thin Film Oven (RTFO) Test

The RTFO test method uses an electrically heated convection oven. This test was conducted by heating a thin film of asphalt binder rotating in the oven for 85 minutes at 163°C. The rotating film was prepared by measuring 35 grams of the asphalt binder sample into RTFO bottles which were then placed in a circular metal carriage that rotates at a rate of 15 revolutions per minute within the oven. The air flow was maintained at 4,000 mL/min [31].

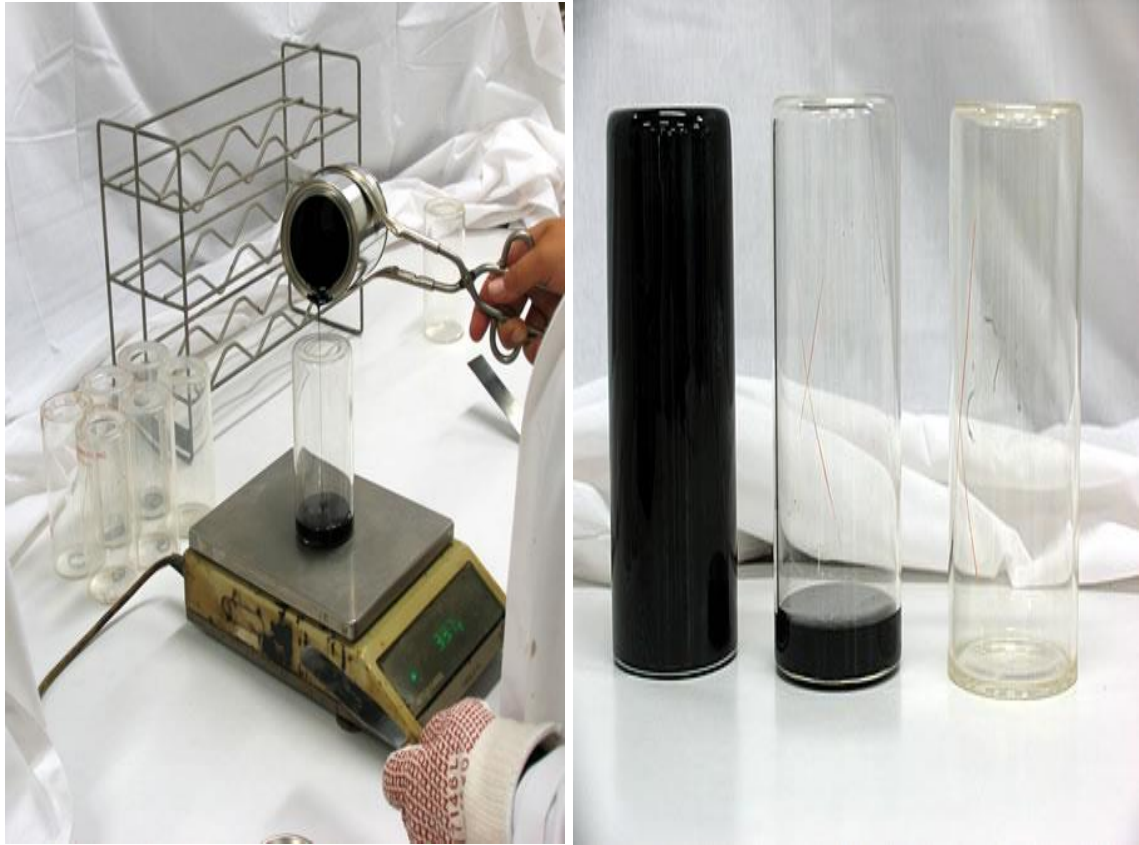


Figure 3.1: Sample preparation for RTFO test [39].

3.1.3 Pressure Aging Vessel (PAV) Test

In this test, several PAV pans are each filled with 50 grams of RTFO-aged binder, arranged in a rack and placed in the PAV. The test was carried out at a temperature and pressure of 90°C and 2.08 MPa respectively for 20 hours.



Figure 3.2: Sample preparation for PAV tests [42].

3.1.4 Recovery of Asphalt Binder from Asphalt Core Samples

Core samples were chopped into pieces and about 5-6 kg of the pieces of specimen were placed in a can. The chopped samples were soaked in toluene and left to stand overnight to ensure complete dissolution of the chopped core samples. The resulting solution of toluene mixed with asphalt binder was then decanted into empty bottles and labelled. The residue left after decanting is washed for several times with toluene and decanted again to ensure that all that was left behind was sediment sand and aggregate.

The toluene-asphalt binder mixture obtained from decanting was then fed into a rotary evaporator to extract the solvent leaving the asphalt binder behind. The extraction of the solvent

was done by condensation using the rotary evaporator. The solvent was condensed between 70 to 80°C and an aspirator pressure set at 180 mbar.

The pressure of the aspirator was gently decreased as the extraction process was ongoing until a point where no more solvent could be extracted. Right after this process, the temperature was set to 200°C under a pressure of 10 mbar for 2 hours to ensure all the solvent has left the asphalt binder. The recovered asphalt binder was then weighed and poured into an empty beaker and was labelled. The percentage of asphalt binder content (% A.C) of the mix was calculated using the equation [25]:

$$\% \text{ A.C} = (\text{weight of recovered asphalt binder} / \text{Total weight of pieces of mix}) \times 100$$



Figure 3.3: A Cole Parmer rotary evaporator [66].

3.2 Dynamic Shear Rheometer (DSR) Method

3.2.1 High and Intermediate Temperature Tests

To evaluate the permanent deformation resistance and fatigue cracking resistance of the recovered and tank asphalt binder samples high and intermediate temperatures respectively, the DSR was used. In this test, the test specimens were prepared by heating the asphalt binder samples in an oven until they became less viscous and easy to pour into silicon molds made for specific dimensions. The dimensions of the samples depend on the type of test to be performed, high temperature (25mm) or intermediate temperature (8mm) tests.

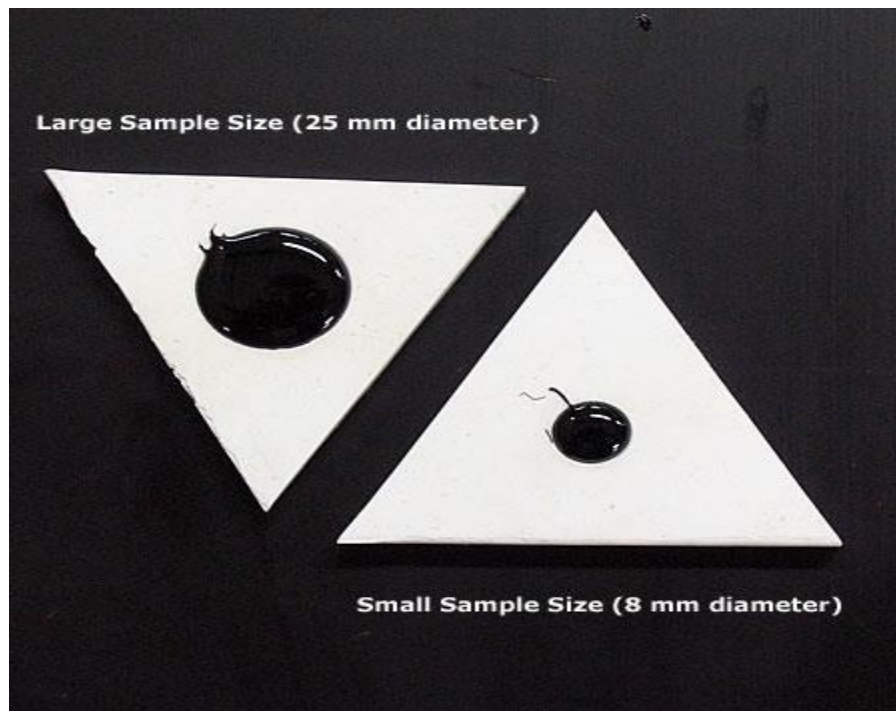


Figure 3.4: DSR samples in silicon molds [67].

The test specimen was the allowed to cool and solidify in the silicon mold before it could be tested. Once proper cooling has occurred and the asphalt binder has taken shape of the silicon mold, the parallel plate geometry of the DSR was heated to 46°C to enable the test specimen to

be attached to the plate prior to testing. A gap zero calibration was performed on the DSR before mounting the test specimen on the plate. The plate was then adjusted until the upper plate slightly touches the surface of the test specimen. Using a trimming tool, the test specimen was trimmed to remove excess asphalt binder stuck to the sides of the parallel plate due to the compression of the plates.

The desired test temperature was set and the test was carried out at a frequency of 10 rad/sec for 10 cycles. The complex shear modulus (G^*) and the phase angle (δ) were recorded by the DSR software during the cycles. The recorded complex shear modulus (G^*) and phase angle (δ) were then used to determine the high and intermediate temperature grading of the samples [31].

3.2.2 Torsion Experiments

Torsion experiments were also carried out on asphalt binder samples at angular frequencies of 0.1, 0.3, 1.0, 3.0 and 10 radians/second at temperatures of 12, 6, 0, -6 and -12°C.

Asphalt binder samples were heated in an oven until they were fluid enough to be poured into silicon molds of desired dimensions (40mm x 12.5mm x 5mm). Tests were done to determine the phase angle (δ), complex shear modulus (G^*), the elastic component (G') and the viscous component (G'') of the asphalt binders.

3.3 Bending Beam Rheometer (BBR) Method

The BBR method was used to assess the propensity of the asphalt binder to undergo physical hardening and thermal cracking. The test specimen (beams) were prepared by heating the various recovered highway asphalt binder samples in an oven until they were fluid enough to pour into molds with definite dimensions.



Figure 3.5: Preparation of BBR beams [46].

The beams of asphalt binder were trimmed immediately after they were properly cooled and had taken the shape of the mold. After trimming, the beams were conditioned in an ethanol bath for 1 hour at $T_{\text{design}} + 10^{\circ}\text{C}$ and $T_{\text{design}} + 20^{\circ}\text{C}$ prior to testing. The beams were then tested at $T_{\text{design}} + 10^{\circ}\text{C}$ and $T_{\text{design}} + 16^{\circ}\text{C}$ in the BBR instrument. A graph of load and deflection versus time was obtained and the instrument automatically measured the creep stiffness (S) and the creep rate

(m). The creep stiffness (S) and the creep rate (m) were used to determine the low temperature grades of the tested asphalt binders [25].



Figure 3.6: BBR beam ready to be tested [46].

3.3.1 Extended Bending Beam Rheometer (EBBR) Method

The EBBR test was developed to evaluate the extent to which an asphalt binder can undergo physical hardening when kept for longer periods at low temperatures. For the EBBR tests, the beams were conditioned in an ethanol bath at $T_{\text{design}} + 10^{\circ}\text{C}$ and $T_{\text{design}} + 20^{\circ}\text{C}$ for 72 hours and tested in the BBR instrument after 1 hour just like the regular BBR method, and again at 24 and 72 hours. Creep stiffness (S) and the creep rate (m) of the asphalt binders were then recorded. An interpolation of the data was carried out using a pass/fail temperature per AASHTO M320 to determine the grade of the asphalt binder [25,43].

3.4 Double-Edge Notched Tension (DENT) Test LS-299

The DENT test was employed to address the fatigue cracking distress observed on asphalt pavements. This test is used to evaluate the ductile failure resistance of asphalt binder when it is pulled apart at a constant loading rate of 50 mm/min at a temperature of 15 °C. The DENT test specimen was prepared by heating the recovered asphalt binder in an oven until it became fluid enough to pour into silicon molds of opposite notches with different notch length of 5 mm, 10 mm and 15 mm. The specimens were then allowed to cool and to take the shape of the mold. The specimens were then taken out of the molds and conditioned in a water bath at a temperature of 15 °C for 3 hours before testing.

The test involves the specimen being pulled at a constant loading rate of 50 mm/min in a water bath of 15 °C temperature until failure occurred. The test was done twice for each different notch length for reproducibility. The Critical Tip Opening Displacement (CTOD), Essential Work of Fracture (EWF) and Plastic Work of Fracture (PWF) were determined using an excel sheet to process the data obtained from the test [25].

3.5 X-Ray Fluorescence (XRF) Analysis

XRF data for the asphalt binder samples were collected using a handheld Brucker Tracer III analyser. This is done to look for the presence of suspect heavy metals. The XRF instrument irradiates the surface of the material with high-energy X-rays, leading to the ejection of inner K-shell electrons from heavy elements. The vacancies this effect produces are then reoccupied by electrons from the outer L- and M-shells. As electrons descend from these outer shells, it is accompanied by the emission of a lower energy X-ray which characteristic of the element being irradiated. The XRF analyser detects the emitted radiation, and a plot of intensity versus the X-

ray energy provides both qualitative and quantitative information on the presence of a range of heavy elements. Peak heights in the spectrum give a quantitative representation of the presence of the metal, but calibrations for each metal need to be done to provide absolute comparisons between metals since fluorescence yields vary between different elements [68].

CHAPTER 4

RESULTS & DISCUSSION

4.1 Extended Bending Beam Rheometer (LS-308) Method

This method is very important for thermal cracking analysis due to its ability to account for physical hardening phenomenon that occurs when asphalt binders are exposed to extremely low temperatures for long periods.

For this study, quality assurance LS-308 data obtained from testing tank samples from 4 different paving contracts from Highway 17, labeled A, B, F and H as well as those from Highways 416, 108, 11, 417 and 6, labeled C, D, E, G and I respectively was compared to LS-308 results obtained for recovered asphalt samples for the same contracts. The recovered samples were taken from two different locations for a given contract.

According to the mix design specification, the asphalt binders being used in this study have minimum performance grade temperature of -34°C . Therefore, as per the LS-308 method, the samples were conditioned at -24°C and -14°C for 72 hours and tested at -24°C and -18°C after 1 hour, 24 hours and 72 hours.

The low temperature grades of both tank and recovered samples (Figure 4.1) was obtained by finding the limiting temperature where stiffness (S) = 300 MPa and the limiting temperature where (m -value) = 0.3 and then performing an interpolation. The limiting minimum temperature grade is the warmest temperature between the two temperatures.

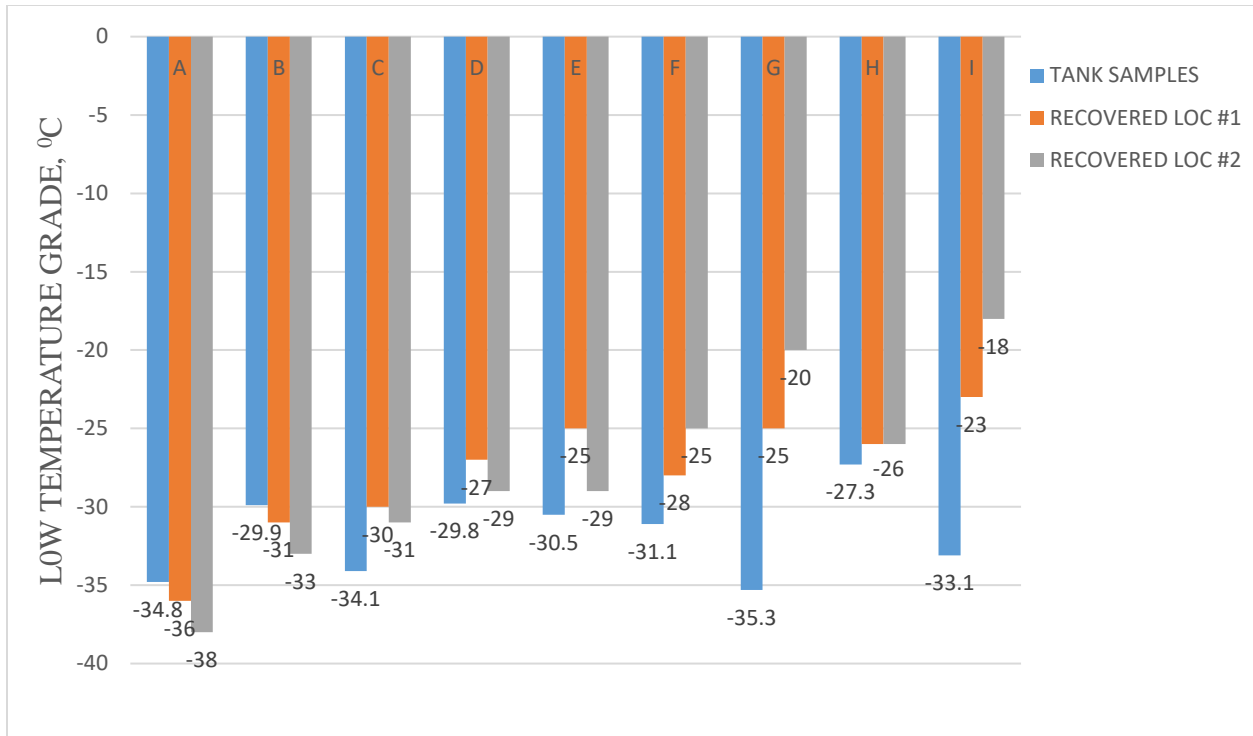


Figure 4.1: Low temperature grades for tank and recovered samples from the same paving contracts.

Tank samples A, C and G are the only quality assurance samples with temperatures lower than the minimum PG temperature given by the mix specification. Hence these are the samples that should be expected to have a good resistance to thermal cracking at temperatures equal to or warmer than minimum PG temperature. The remaining 6 tank samples fall short of the minimum PG temperature, each by different degrees. These 6 tank samples cannot be expected to exhibit good resistance to thermal cracking resistance at the given mix design PG temperature. Among the tank samples, the worse off asphalt binder is that of sample H, whose low temperature grade is -27.3°C (about 7°C warmer than the minimum PG temperature).

It is also interesting to note that except for the recovered samples A, none of the recovered samples for the same contracts seem to meet the minimum PG temperature, and are even worse

off than their corresponding tank samples in almost all cases, with only sample B being the exception in this category. Of all the recovered samples tested, sample I recovered from location number 2, showed the worst degree of deviation from the expected performance grade in reference to the mix design specification, with a minimum PG temperature of -18°C , with sample G recovered from location number 2 following suit with a -20°C PG temperature.

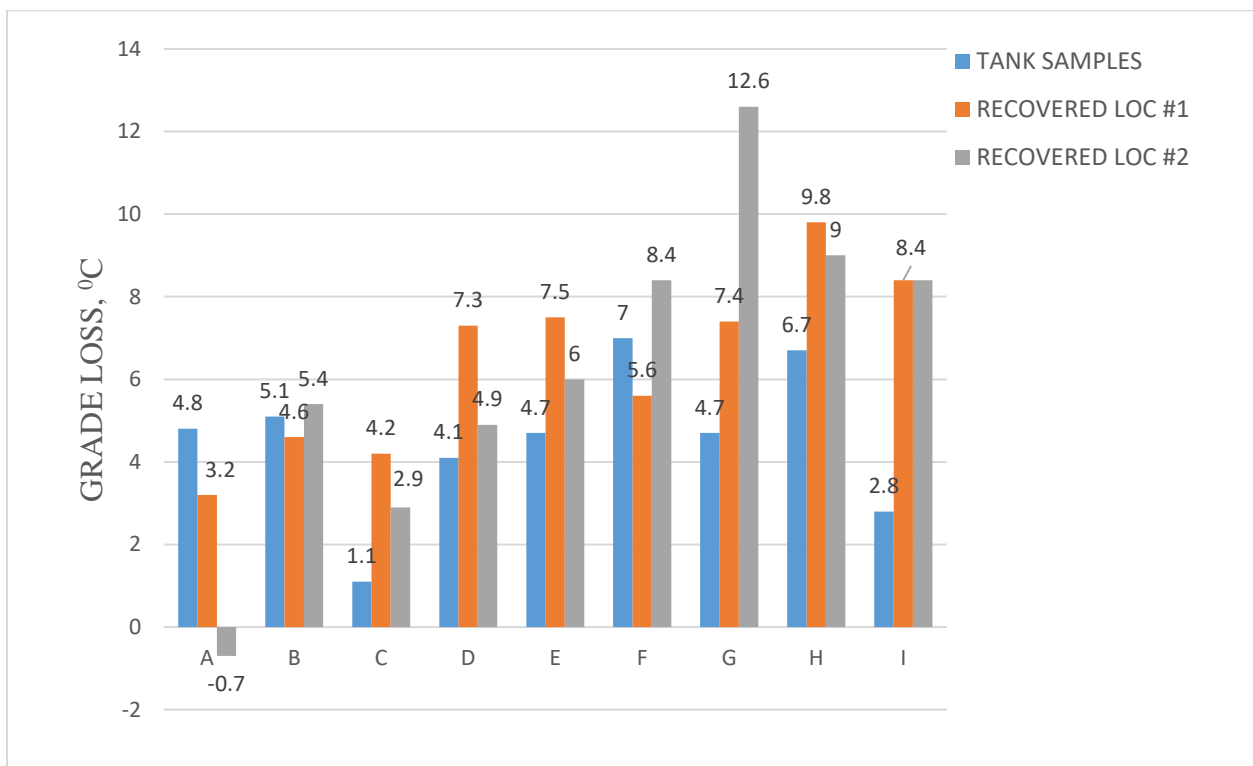


Figure 4.2: Grade loss in tank and recovered asphalt samples from the same paving contracts.

Grade loss is a parameter that gives a good indication of how asphalt binders will respond to thermal stress and physical hardening. In other words, it helps to know or predict the in-service performance of asphalt binders. Asphalt binders that exhibit less grade loss after 72 hours of

conditioning and testing in the BBR as per the LS-308 protocol, indicates that the asphalt binders under study have good resistance to physical hardening and is able to relax thermal stresses that occur in the asphalt pavement more quickly compared to asphalt binder samples with more grade loss. This consequently means, less or no stress during “spring thaw” and hence less or no cracking [69].

Looking at Figure 4.2, we see both tank and recovered samples exhibiting significant grade losses, once again some to a larger extent than others. Again, it is interesting to see with a few exceptions, most of the recovered samples experiencing larger grade losses relative to their corresponding tanks samples. Some of these differences are so pronounce, an example being contract G where the comparison between tank sample and recovered sample from location number 2 show a grade loss difference of 7.9 °C.

These differences make one wonder what the issue might be and draws attention to the need for further investigation with the following questions in mind:

- Why are there such significant differences between data obtained for quality assurance tests done on tank samples and the test results for recovered samples?
- Is there perhaps a difference between the asphalt binder samples that undergo quality assurance tests and the asphalts binders actually used in road construction?
- What happens to the asphalt binders between the time quality assurance tests are performed and when road construction takes place?

Before any conclusion are made, data from other testing protocols need to be analysed to be sure if suspicions are valid.

4.2 Double Edge Notched Tension Test LS-299

For this test, the concept of essential work of fracture (EWF) is used to investigate the ductility of asphalt binders and consequently determine their strain tolerance and failure properties [26].

The use of this concept was validated as a simple failure test for asphalt binders by Andriescu et al in 2004 and 2006 [70].

The ductility of the asphalt binders was investigated by stretching them at a rate of 50mm/min in an isothermal water bath at 15 °C until failure occurs. This method provides a good distinction between poorly performing asphalt binders and superior ones.

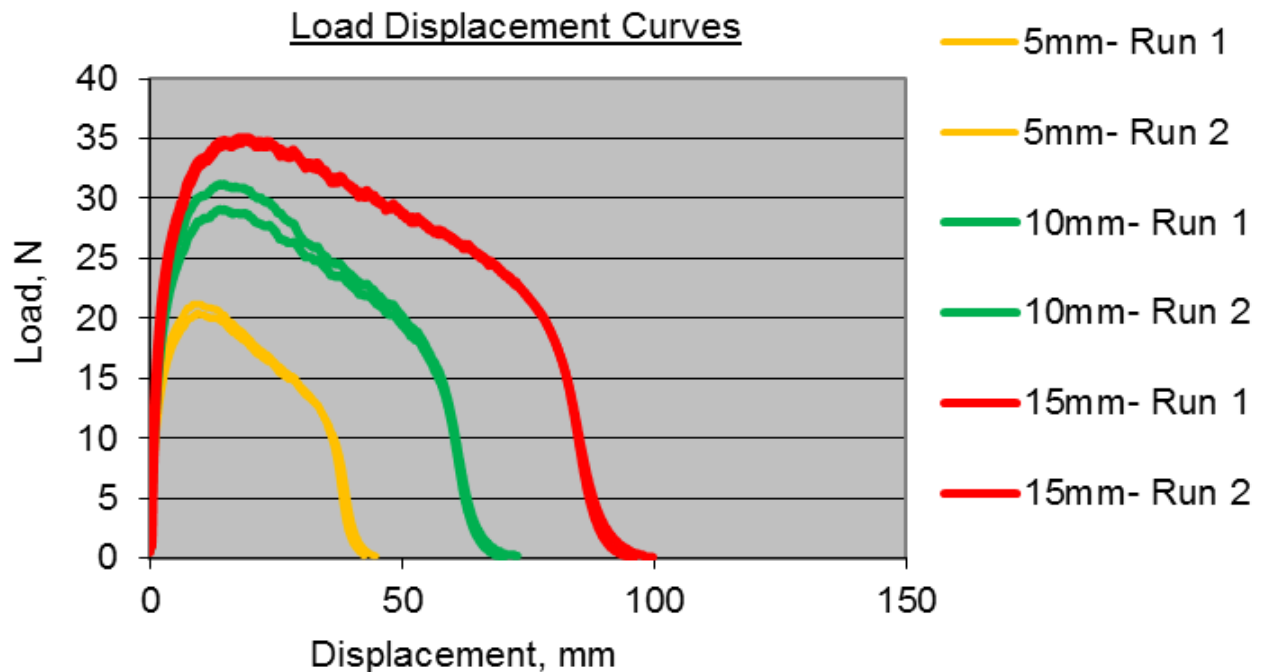


Figure 4.3: Force-Displacement curves for sample C for various ligament lengths.

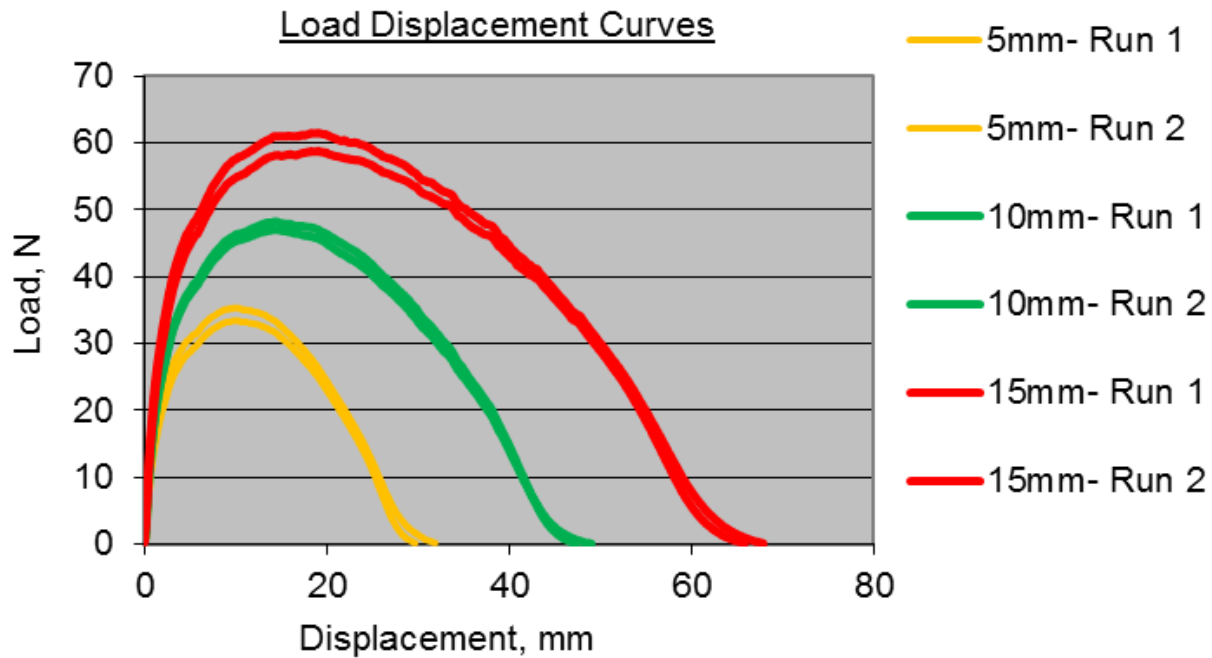


Figure 4.4: Force-Displacement curves for sample D for various ligament lengths.

Figures 4.3 and 4.4 are testament to the reproducibility of this test method with similar measurements for same ligaments lengths but different curves the different types of asphalt binders. This information is important because in order for EWF measurements to be valid, all specimen need to go through the same sequence of stretching, yielding and then tearing [59].

EWF values are generally expected to be high since it is thought that fatigue cracking occurs only when the strain tolerance of the asphalt binder is exceeded. Hence the higher the EWF value of the asphalt binder, the more resistant it is to fatigue cracking [24]. It is also important to note that EWF is considered a material property and therefore is not dependent on the geometry of the asphalt binder [12].

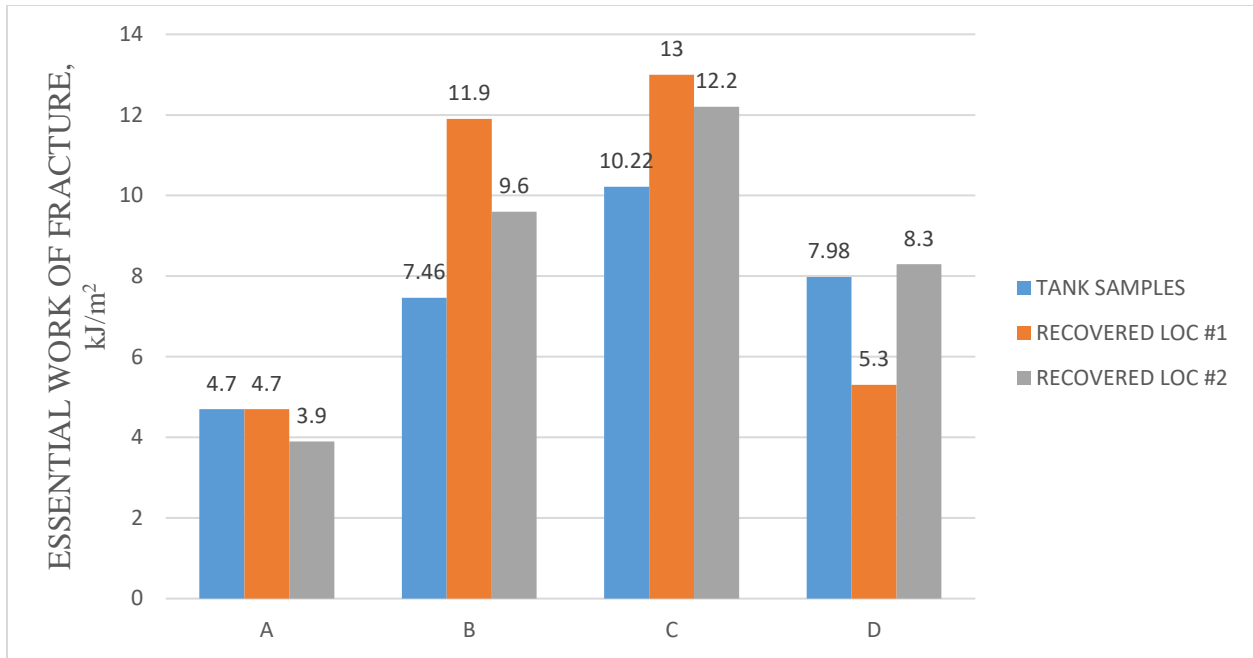


Figure 4.5: Effective work of fracture of tank and recovered samples

Figure 4.5 shows EWF values for tank and recovered samples of four of the different paving contracts outlined in this study. Here the recovered samples are showing either similar (as shown by contract A) or higher values of EWF compared to their corresponding tank samples. This effect means they are exhibiting better strain tolerance compared to the tank samples and hence are less susceptible to fatigue cracking.

A look at the plastic work of failure, which is a non-material property but nonetheless gives some idea about fatigue cracking, shows similar trends (Figure 4.6) to those in Figure 4.5. Plastic work of failure is the energy associated with causing non-essential deformation that falls outside the fracture zone of the asphalt binder [25]. Just like the EWF, the higher the value of the plastic work of failure, the better, since high plastic work of failure is associated with high asphalt binder content in the asphalt cement which bodes well for fatigue cracking resistance [61]. In Figure 4.6, except for contract A, in which the plastic work of failure in the tank sample seems to

be higher than the recovered samples, the other contracts seem to exhibit either the same (as in the case of contract D) or higher plastic works of failure for the recovered samples compared to the tank samples.

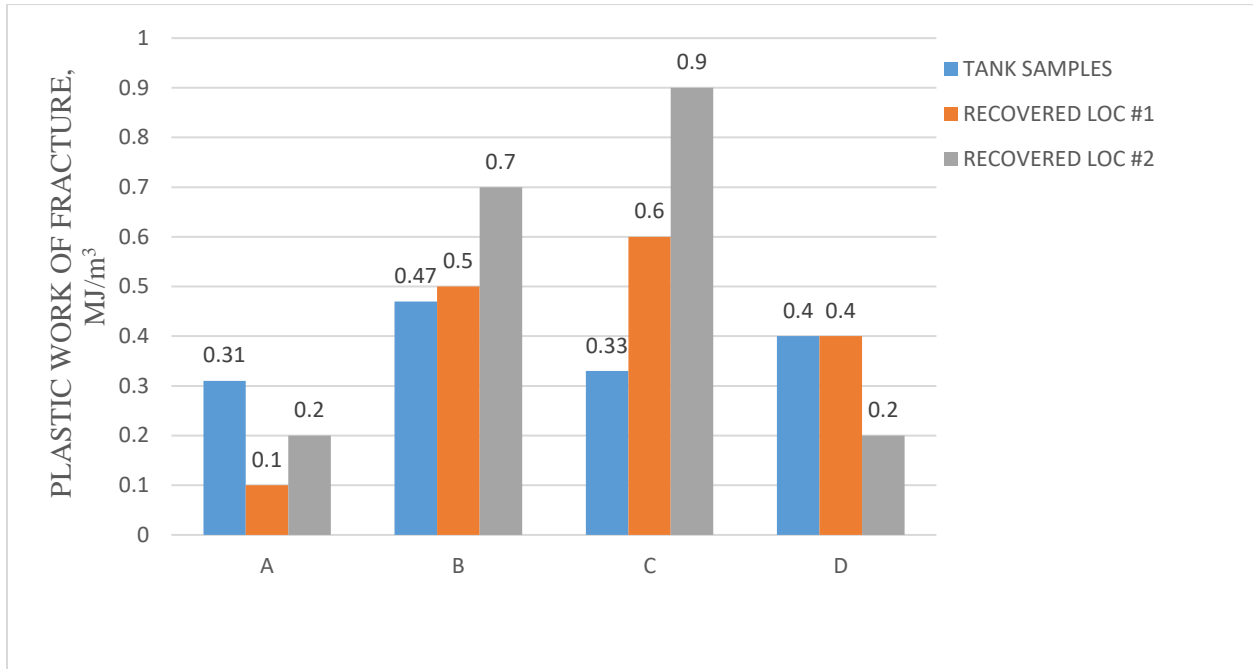


Figure 4.6: Plastic work of failure for tank and recovered samples.

Finally, we look at the CTOD which is directly related to the essential work of fracture and provides a way to measure strain tolerance in the ductile state under high levels of constraint. CTOD essentially measures how much a thin fiber of asphalt binder can be stretched before it fails. This has an inverse relationship with the amount of distress [71]. CTOD also gives a much more precise measure of fatigue cracking resistance compared to the plastic work of failure and EWF measurements. Also, as with the case of the plastic work of failure and EWF, the higher the CTOD value the better the strain tolerance and lower the susceptibility to fatigue cracking [29,70].

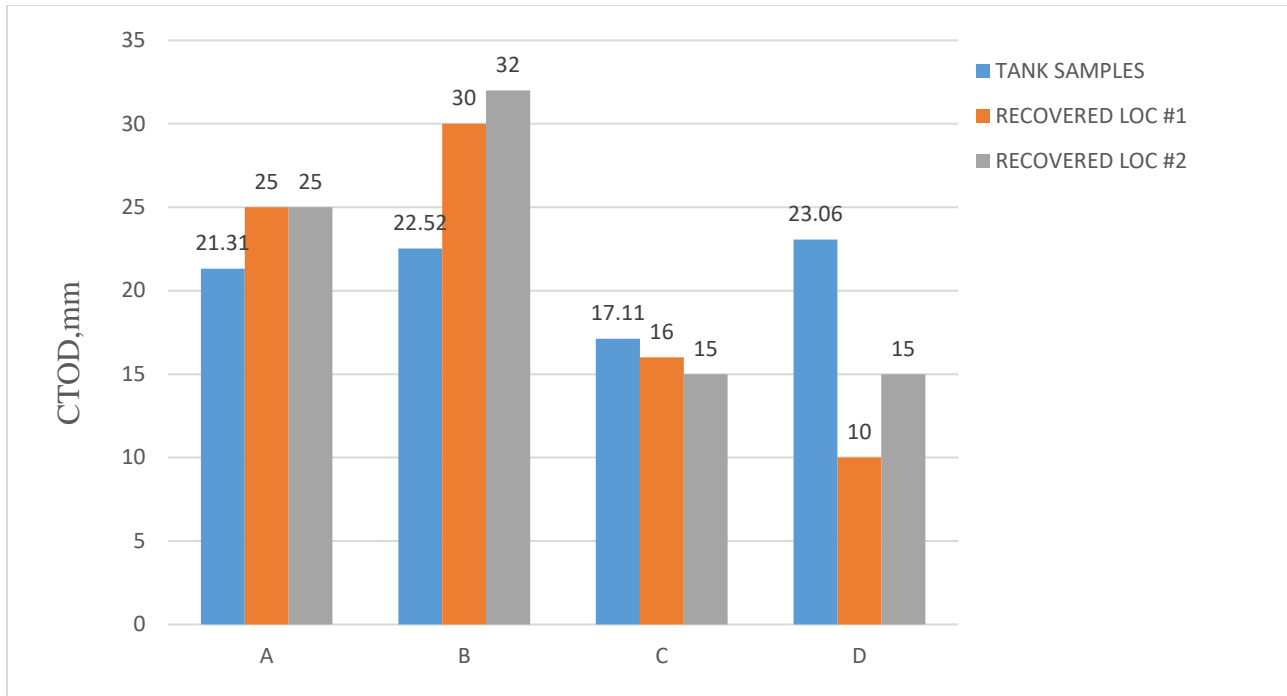


Figure 4.7: Crack Tip Opening Displacement measurements for tank and recovered samples.

For the CTOD measurements in Figure 4.7, contracts A and B show higher CTOD values for recovered asphalt binder samples compared to their corresponding tanks samples. However, contracts C and D seem to show trends completely opposite to what is seen for contracts A and B. Here, we observe that the tank samples have higher CTOD values compared the recovered samples, implying that the tanks samples have higher resistance to fatigue cracking. However, according to the LS-299 protocol, the CTOD acceptance limit for a PG-34 asphalt binder is 20 mm [72]. Based on this, both tank and recovered samples for contract C has failed the DENT tests. Once again, we see a sharp contrast between CTOD values for tank and recovered samples, with tank samples passing the criteria while recovered samples fail miserably (contract D).

The results from the DENT tests have been anything but conclusive, showing varying trends in performance based characteristics for both tank and recovered samples. This perhaps calls for an

investigation into the chemical compositions of the asphalt binders used in the selected paving contracts.

4.3 X-Ray Fluorescence (XRF) Analysis

Based on work done by Hesp and Shurvell [68] in which waste engine oil (WEO) was found in asphalt pavements across Ontario, XRF analysis was carried out on both tank and recovered asphalt binder samples to discover as well as compare the relative amounts of heavy metals which could be indicative of WEO or other types of additives/modifiers. From their research, they discovered that the presence of heavy metals especially zinc, was indicative of the presence of WEO as an additive in the asphalt binders. The presence of WEO was inferred to be the cause of increased chemical and physical hardening of asphalt binders [68].

The heavy metals in WEO destabilize the asphaltenes in the asphalt binder, causing changes in chemical properties, which in turn leads affects its rheological performance badly. Also, the paraffinic nature of WEO leads to increased precipitation of asphaltenes causing a decrease in the adhesive strength of the asphalt binder to the aggregate, which may result in stripping and consequently rutting [10,25].

Hesp and Shurvell [68] performed X-ray analysis on asphalt binders from 26 different asphalt pavement contracts. Results showed that 12 out of 15 poorly performing asphalt pavements had significant amounts of zinc in their asphalt binders. According to Hesp and Shurvell, “zinc dialkyldithiophosphate (ZDDTP) is a universal and deliberate antioxidant and anti-wear additive in engine oils, and zinc is therefore expected to be present in these residues in relatively constant amounts” [68]. However, the 11 superior performing asphalt pavements showed no sign of zinc. They therefore concluded that, the presence of WEO residues in asphalt pavements is the cause of unexplained premature and excessive cracking and consequently failure of Ontario road

networks and this is largely due to the increased physical hardening and reduced strain tolerance this additive causes [68]. In this research, both tank and recovered asphalt binder samples from the same contract undergo XRF analysis to determine the amount of heavy metals present in each of these samples and the data obtained is compared to support data from physical performance tests done earlier in this study.

Table 4.1: XRF data for tank samples from 4 different paving contracts in Ontario recorded as peak heights in counts/second.

CONTRACT	Zn	Mo	Cu	Ca	S	V	Ni
A	5.5	7.1	28.5	22.9	343.0	76.1	175.0
B	297.4	19.3	40.4	65.0	299.4	37.5	165.9
C	213.9	17.3	35.0	54.8	370.5	37.9	164.6
D	332.3	24.3	38.9	75.0	304.6	40.1	165.2

Table 4.2: XRF data for recovered samples from 4 different paving contracts (8 separate locations) in Ontario recorded as peak heights in counts/second.

CONTRACT	SAMPLE	Zn	Mo	Cu	Ca	S	V	Ni
A	RECOVERED LOC #1	6.1	6.6	32.9	39.3	304.8	65.2	132.3
	RECOVERED LOC #2	5.3	4.8	31.6	44.1	315.6	70.1	131.8
B	RECOVERED LOC #1	98.1	11.6	37.2	75.5	270.6	34.5	134.1
	RECOVERED LOC #2	111.1	13.6	40.5	73.2	272.0	36.9	132.8
C	RECOVERED LOC #1	25.6	6.7	27.1	567.0	337.8	34.6	137.4
	RECOVERED LOC #2	18.4	9.6	27.3	501.6	319.9	34.7	128.5
D	RECOVERED LOC #1	117.4	10.0	41.0	116.8	274.7	34.7	137.3
	RECOVERED LOC #2	141.8	15.0	41.6	111.0	290.2	39.5	141.9

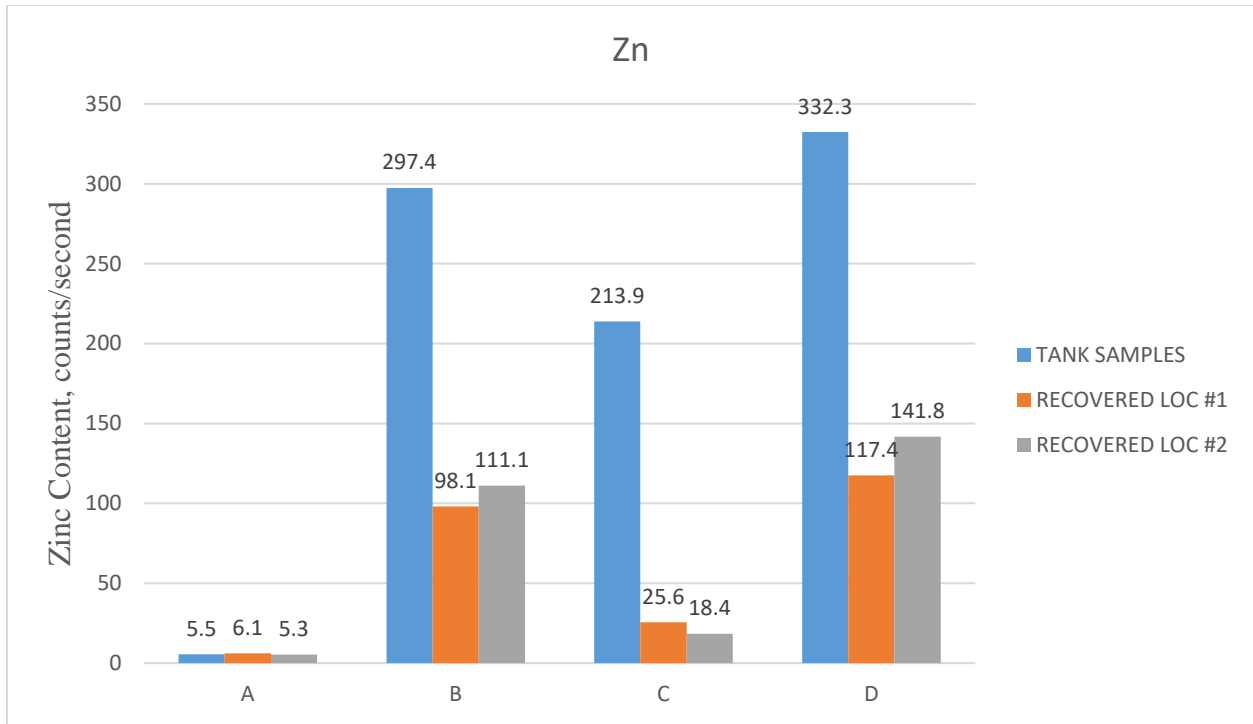


Figure 4.8: Zinc content of tank and recovered samples in counts/second.

XRF analysis recorded high amounts of zinc in the tank samples of contracts B, C, and D with extremely small amounts recorded for contract A (Figure 4.8). The amount of zinc in tank samples for contracts B, C and D however, seems to have reduced by about 50% in the corresponding recovered samples. This could be the result of leaching of the zinc into the lower core layers or into the soil layers below the pavement but this conclusion is purely speculative.

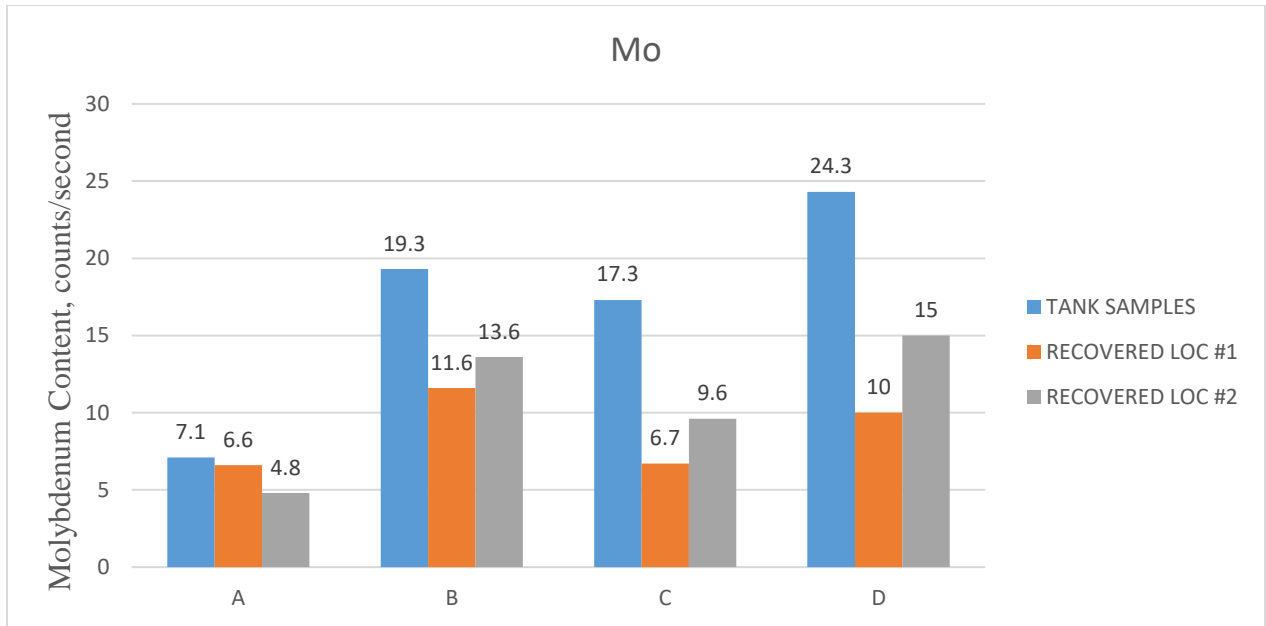


Figure 4.9: Molybdenum content of tank and recovered samples in counts/second.

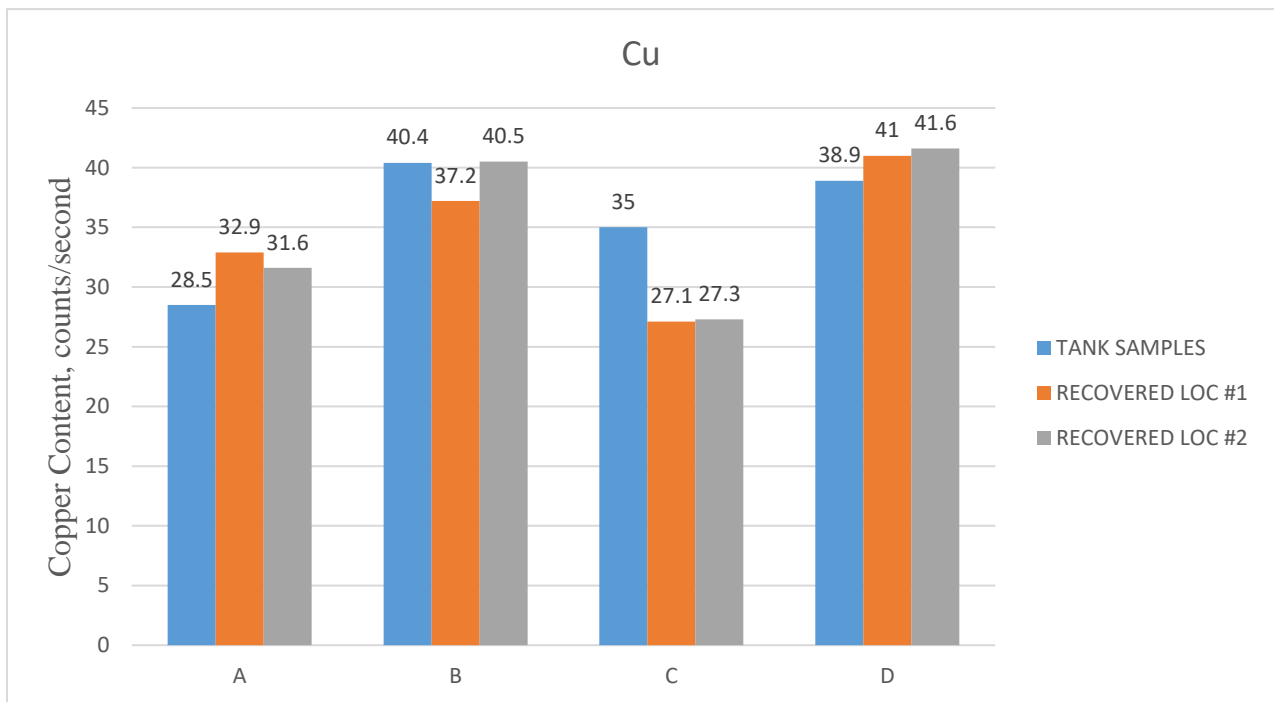


Figure 4.10: Copper content of tank and recovered samples in counts/second.

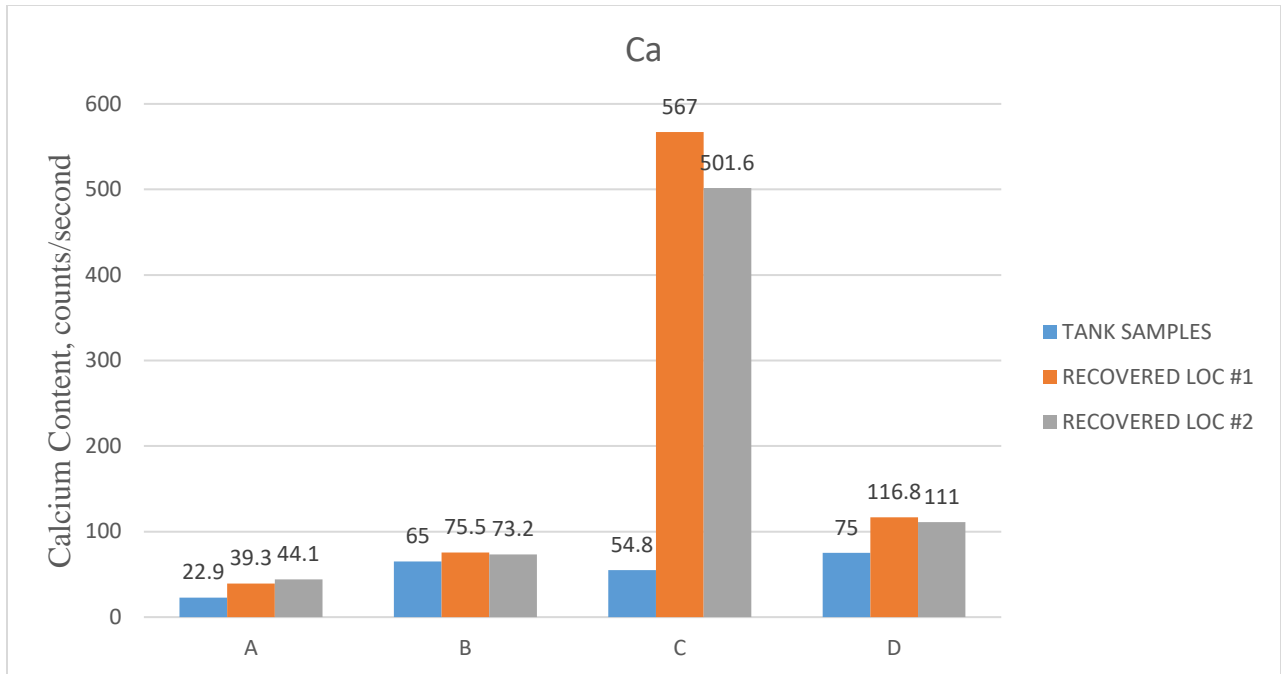


Figure 4.11: Calcium content of tank and recovered samples in counts/second.

Figure 4.11 generally shows high counts of calcium in recovered samples compared to tanks samples. However, for contract C, the recovered sample contains about ten times the amount of calcium in the tank sample in counts/second. This could either be from the aggregate or due to the addition of antioxidants which usually contain calcium salts [73], however it could be something completely different. The point here is that, there is something going on the needs to be addressed. The composition of the asphalt binders being severely altered after quality assurance tests have been conducted seems odd and suspicious, especially if the road networks are failing prematurely or the recovered asphalts binders from these contracts are not meeting the performance grade standards they did during quality assurance tests.

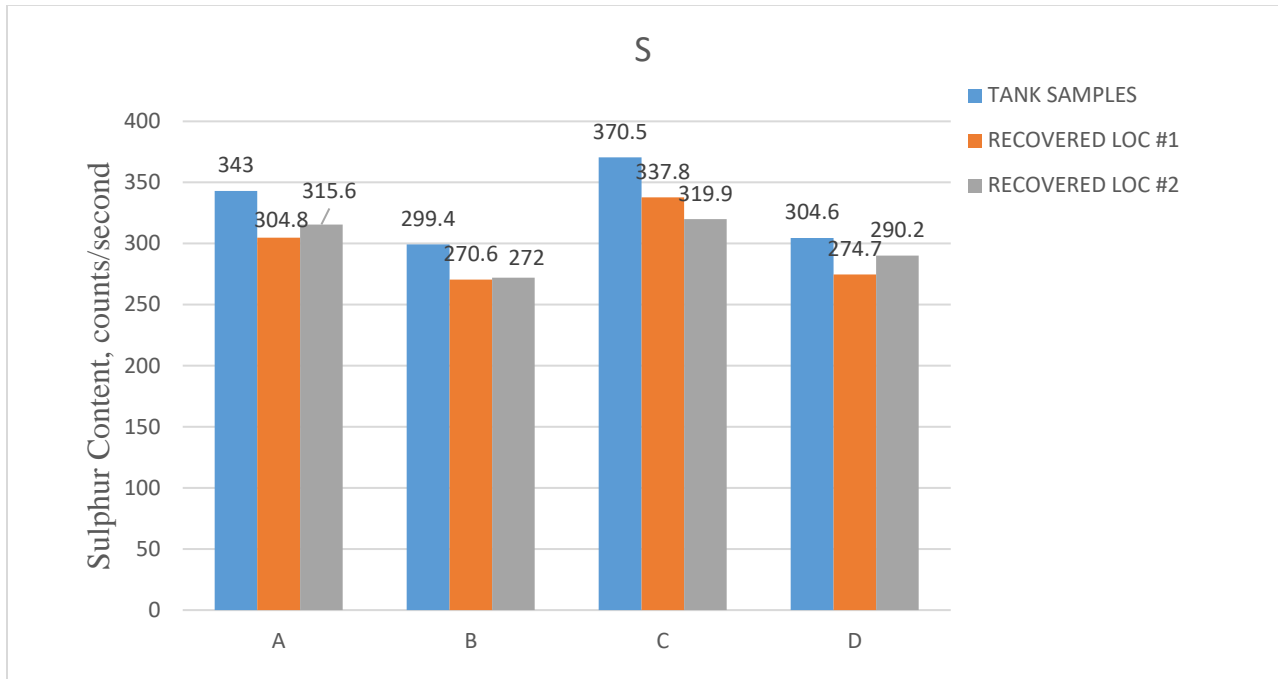


Figure 4.12: Sulphur content of tank and recovered samples in counts/second.

High sulphur contents observed in Figure 4.12, may be due to the use of sulphur as an extender. Extenders are used to reduce the amount of asphalt cement required and this is done by substituting a portion of the asphalt cement [73]. Vanadium (Figure 4.13) and nickel (Figure 4.14) occur naturally in asphalt.

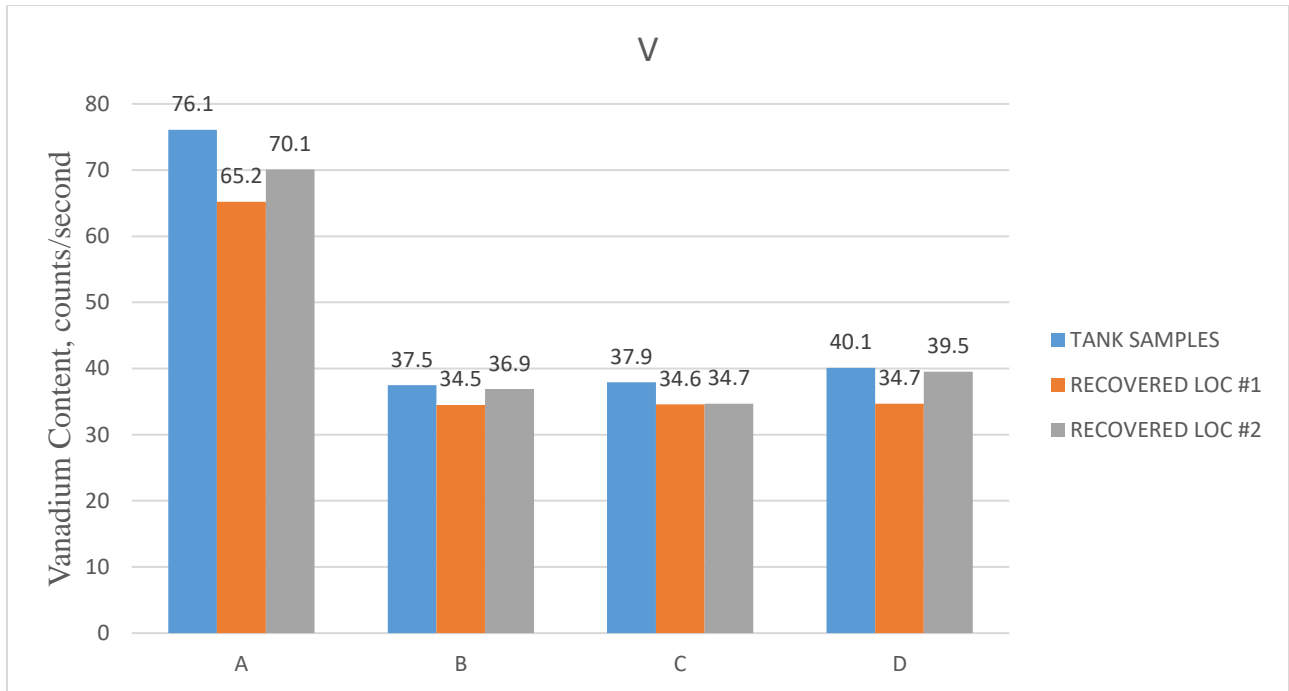


Figure 4.13: Vanadium content of tank and recovered samples in counts/second.

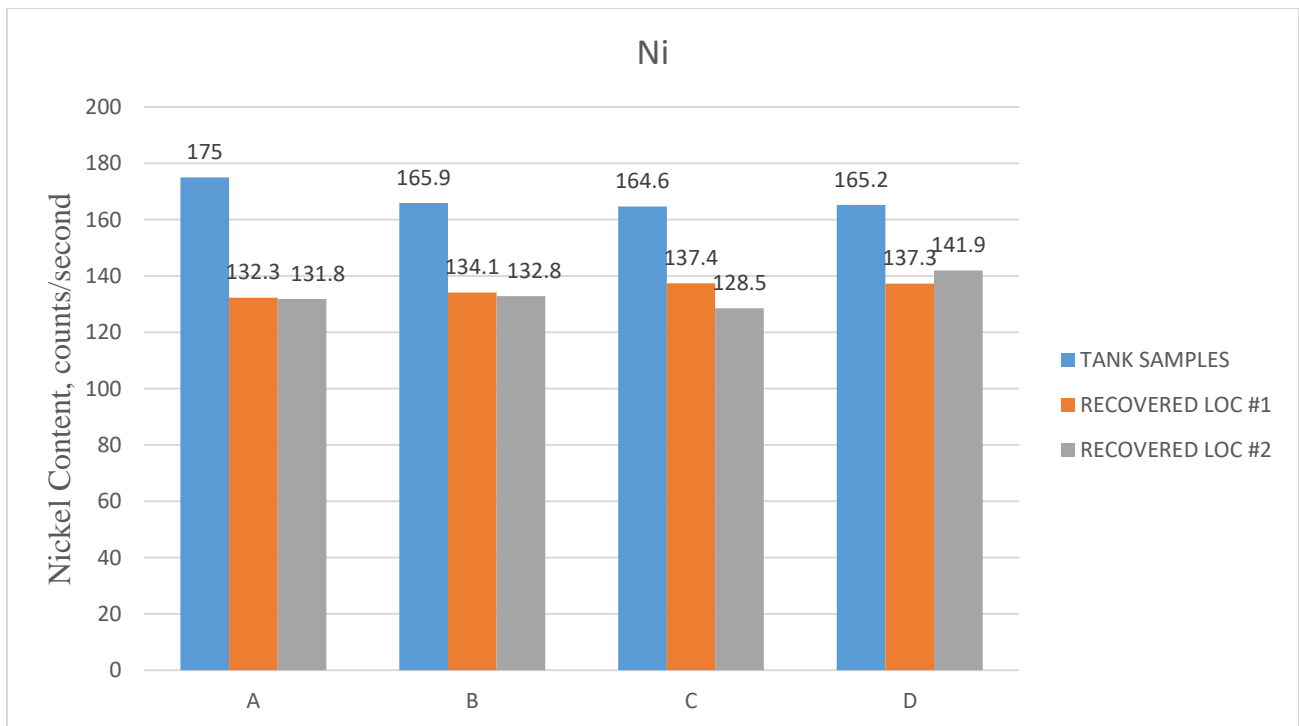


Figure: 4.14: Nickel content of tank and recovered samples in counts/second.

4.4 Dynamic Shear Rheometer Analysis

Figure 4.15 show the limiting maximum temperature PG (high temperature grades) of tank and recovered samples for four different paving contracts after testing in a DSR. The limiting maximum temperature PG represents the temperature at which the rutting resistance factor ($G^*/\sin\delta$) has a minimum of 1.0 kPa for unaged samples and 2.20 kPa for RTFO-aged samples. The higher the high temperature grade, the higher the asphalt binder's resistance to rutting and consequently the better its performance in high temperature climate regions.

According to Figure 4.15, the recovered samples generally have a better resistance to rutting compared to their corresponding tank samples. This implies that the recovered samples demonstrate more elastic and less viscous behaviour in comparison to the tank samples.

Whatever modification may have been done to the asphalt binder after quality assurance tests had been carried out had a positive effect on the limiting maximum PG.

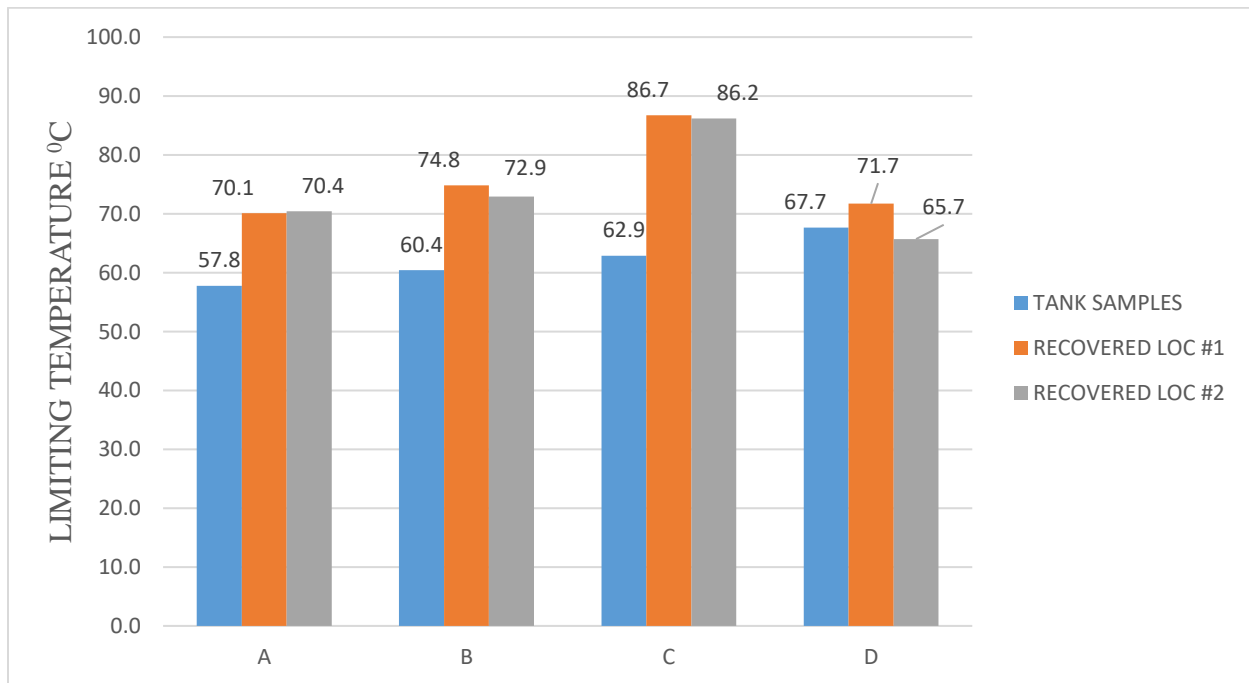


Figure 4.15: High temperature grades of tank and recovered samples.

However, looking at Figure 4.16, it is observed that the recovered samples of contracts C and D seem to be under-designed for intermediate temperature regions compared to their corresponding tank samples. The Intermediate temperature grade is given by the temperature at which the fatigue cracking resistance factor ($G^*\sin\delta$) is less than 5000 kPa for PAV-aged samples. The lower the intermediate temperature of the asphalt binder, the less susceptible it is to fatigue cracking. It is important to note that this measure of resistance to fatigue cracking is not as accurate as the CTOD measurements done in the DENT test. That notwithstanding, for this test, tank samples for contracts C and D are showing less susceptibility to fatigue cracking compared to their corresponding recovered samples. For contracts A and B however, the exact opposite is seen.

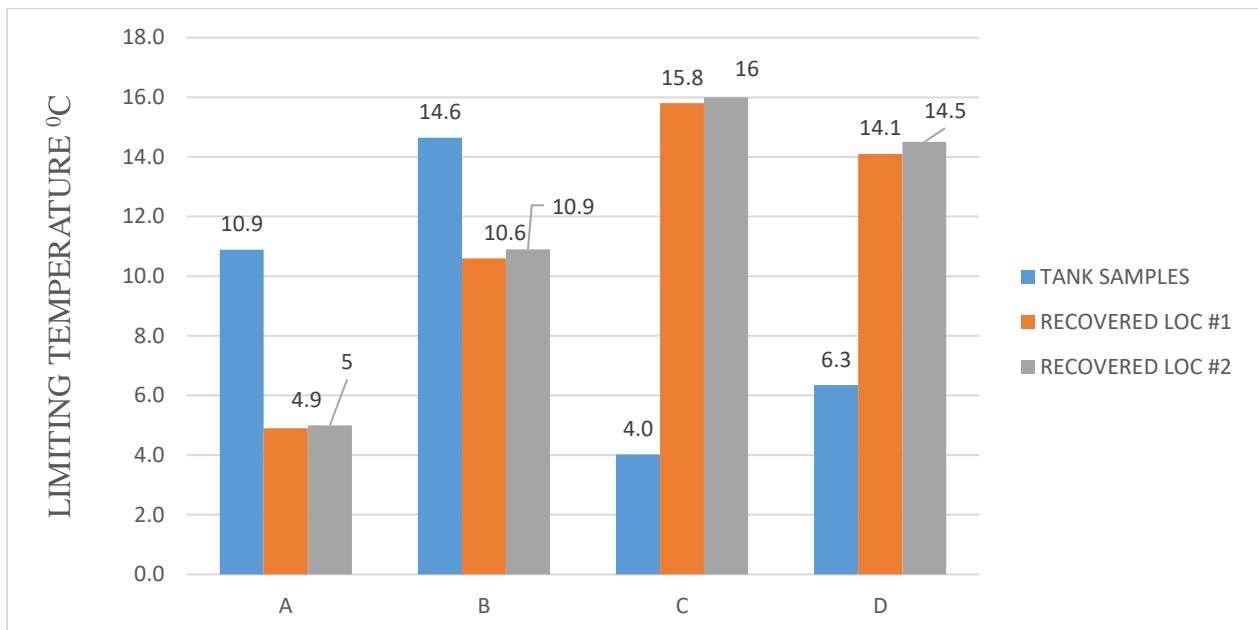


Figure 4.16: Intermediate temperature grades of tank and recovered samples.

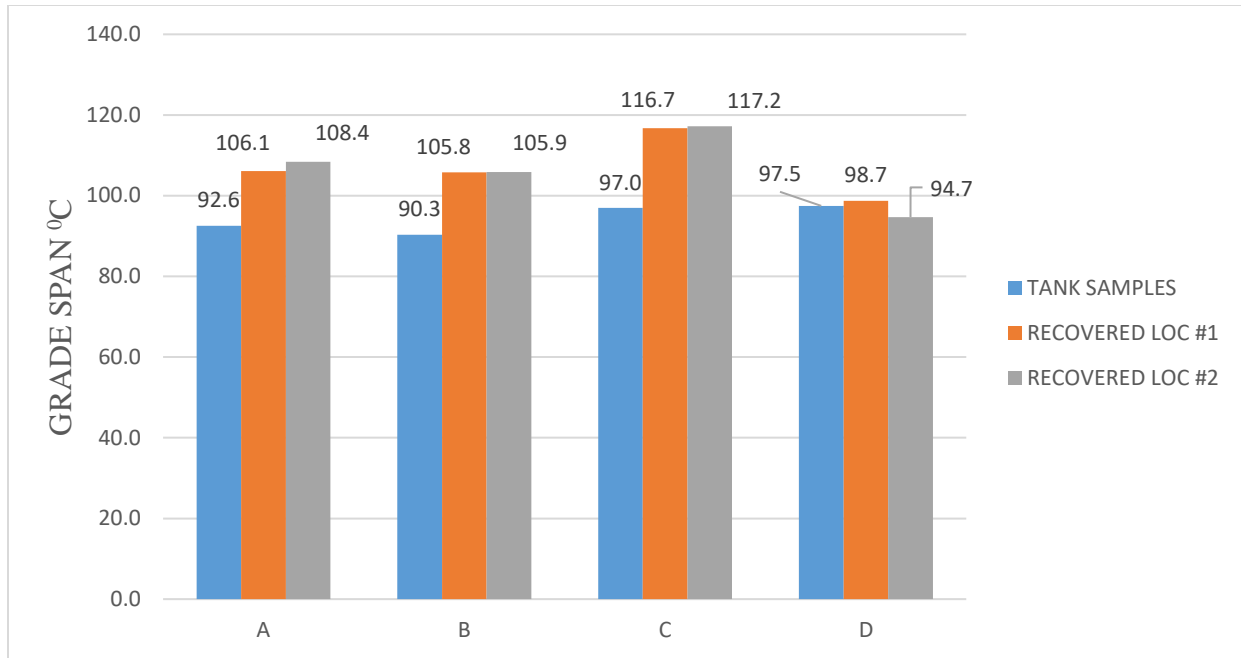


Figure 4.17: Grade Span for tank and recovered samples.

With the exception of contract D, Figure 4.17 shows the grade span for the recovered samples are higher than those of the corresponding tank samples. The grade span is the difference between the limiting maximum performance PG and the limiting minimum PG. Here, the higher the grade span value, the better, since that indicates the asphalt binder will exhibit good performance in climatic regions with a wide range of temperatures.

4.4.1 Torsion Bar Experiments

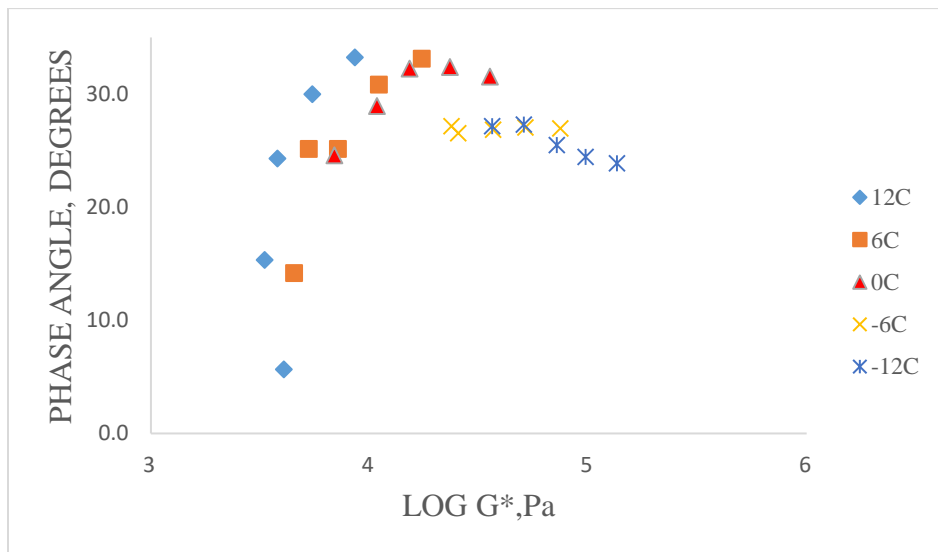
Torsion bar experiments can be used to evaluate the effects of physical hardening on the low temperature rheological properties of asphalt using the DSR [74]. Based on previous work, it was discovered that measuring phase angles at low temperature can help predict thermal cracking in asphalt binder samples. This method was thought to be quite convenient since the procedure is automated and requires relatively short conditioning time [54].

Based on this, a different aspect of this study looks at Black space diagrams from data obtained from torsion bar experiments done on recovered asphalt binder samples from 4 different contracts. Also, comparisons were made between stiffness values measured after one hour testing in the BBR and phase angles obtained from these experiments.

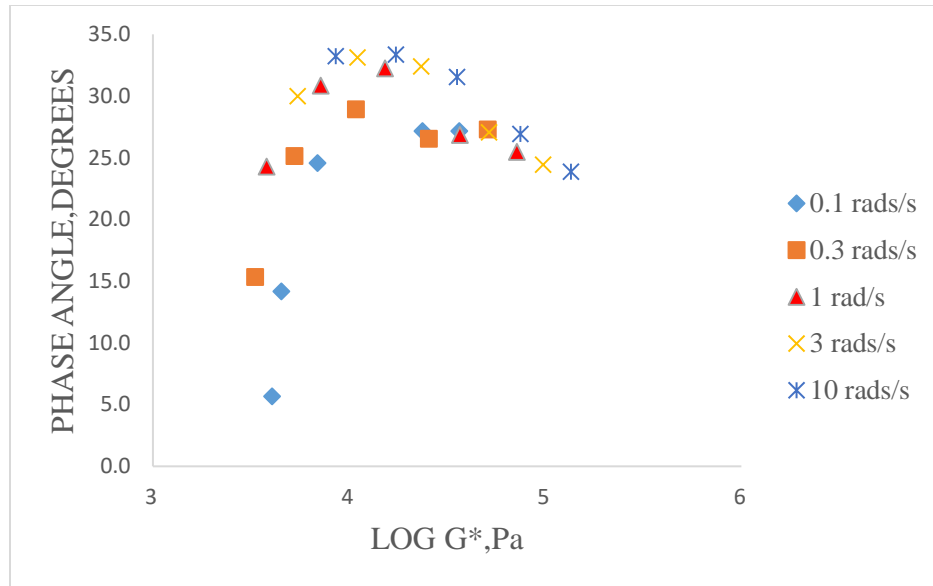
4.4.1.1 Black Space Diagrams

Work done by King et al. [24] suggested that location on Black space diagrams at lower temperatures can be used to better predict cracking and the related failure mechanisms that usually come with highly oxidized asphalt. Regarding binders, the study found that the black space an important performance measure for cracking.

Black space diagrams are simply rheological plots of G^* (modulus) versus phase angle. The diagrams also consider phase changes in the asphalt binder such as wax crystallization, which has been known to lead to physical hardening [24].

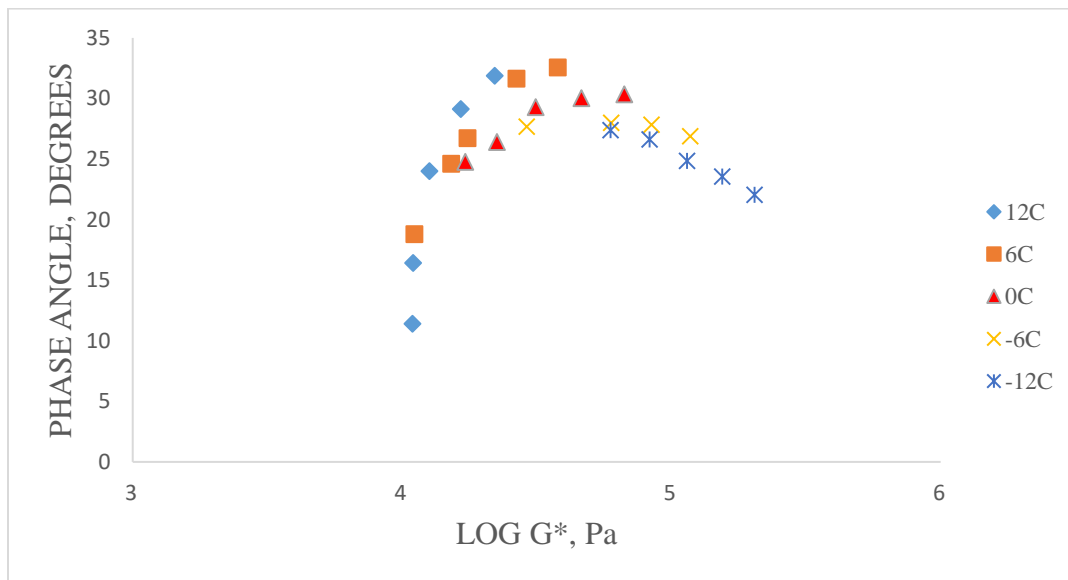


(a)

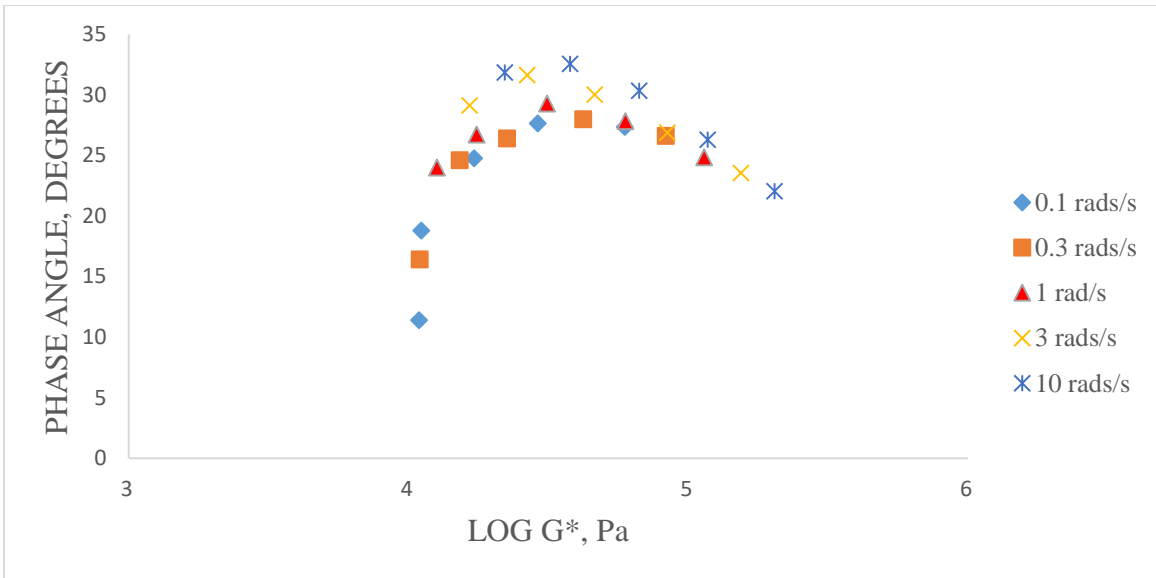


(b)

Figure 4.18: Black space diagram for contract J samples at different temperatures (a) and frequencies (b).

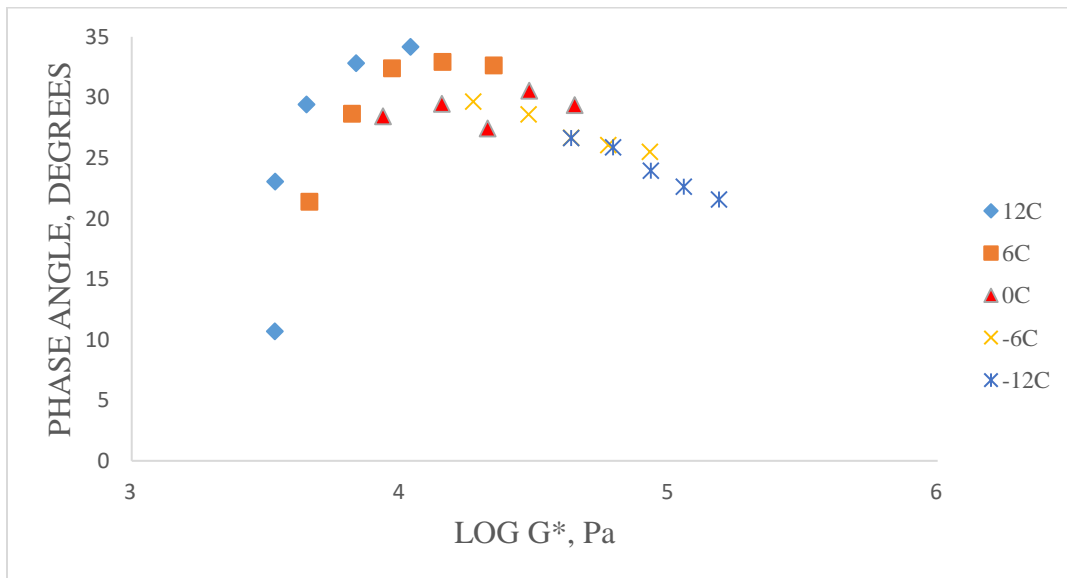


(a)

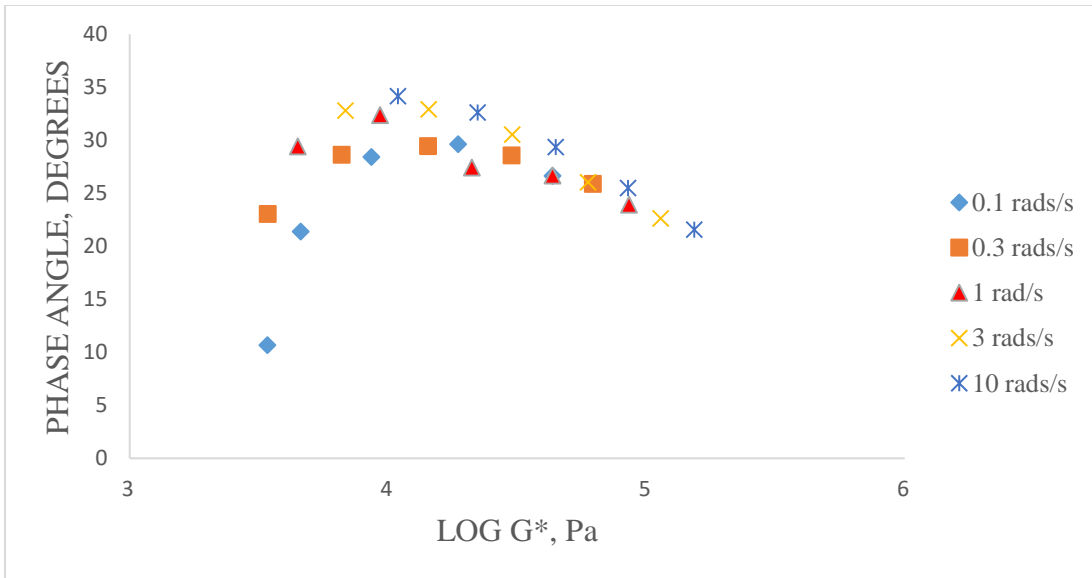


(b)

Figure 4.19: Black space diagram for contract K samples at different temperatures (a) and frequencies (b).

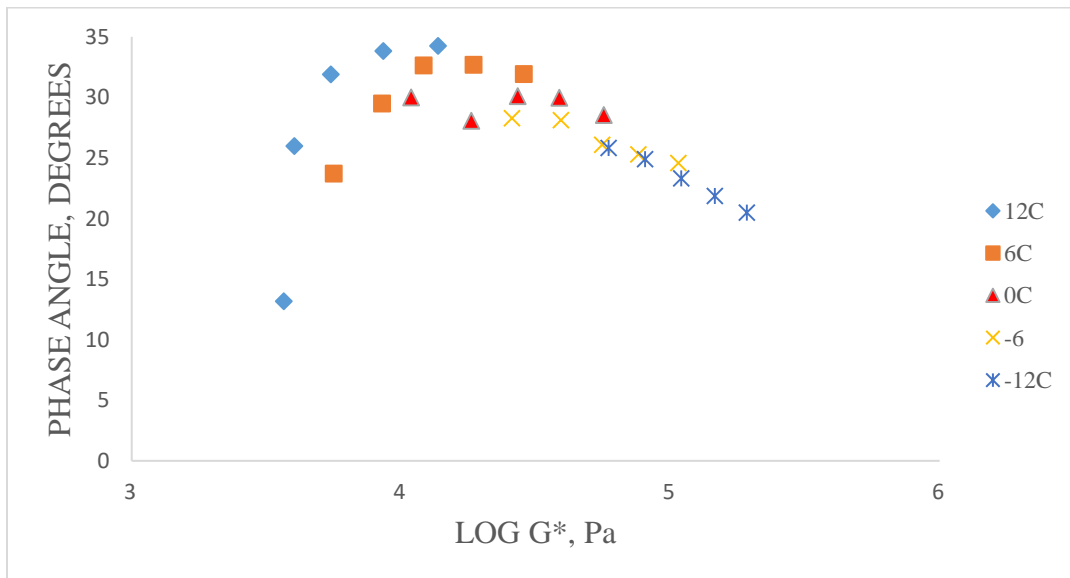


(a)

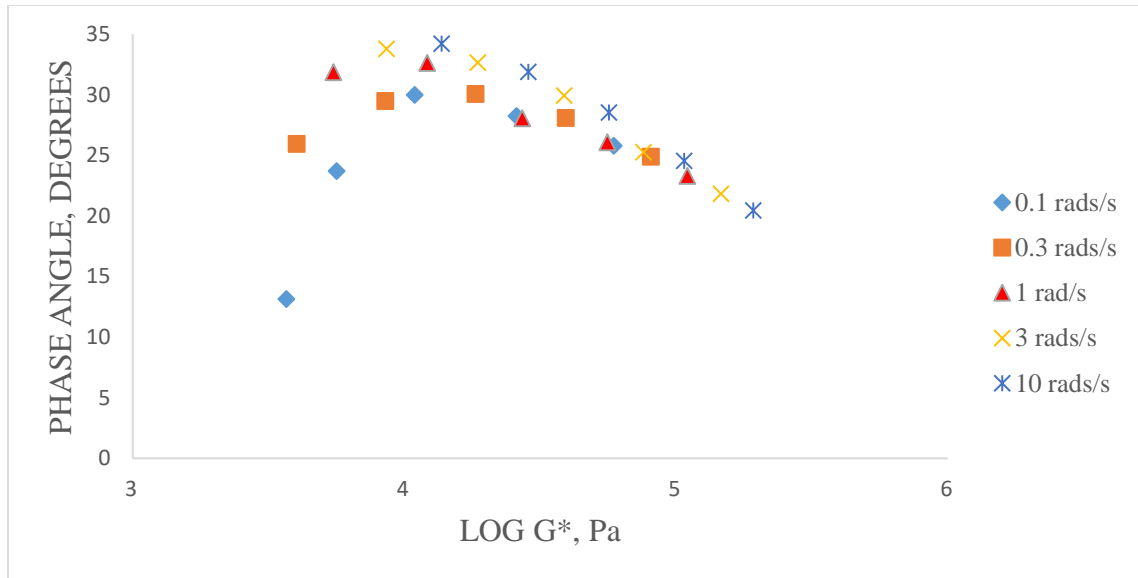


(b)

Figure 4.20: Black space diagram for contract L samples at different temperatures (a) and frequencies (b).



(a)



(b)

Figure 4.21: Black space diagram for contract M samples at different temperatures (a) and frequencies (b).

Looking at the Black space diagrams above, the general trend appears to be a steady increase in phase angle values from 12 °C to around 0 °C. However, at temperatures lower than the 0 °C, the phase angle values begin to reduce. This could be attributed to physical hardening which is known to be prominent below 0 °C because of wax crystallization or gel formation that occurs at extremely low temperatures.

A similar trend is also observed with increasing angular frequency for the temperature, phase angles increase steadily as angular frequency increases above 0 °C but slowly decrease with increasing angular frequency below 0 °C.

Torsion bar experiments done by Freeston et al. [54], found that the best performing asphalt binder samples were those that had high phase angle values after performing torsion bar experiments on samples that had passed other asphalt binder performance tests and those that had failed those tests. The samples that had failed prior performance tests had comparatively low phase angles [54]. Also, asphalt binders with high stiffness and low phase angles are known to perform poorly.

The trend of decreasing phase angles as temperature drops has already been ascertained, however “the final nail in the coffin” will be to take a look at the stiffness values for the samples of the contracts in question after just 1 hour of conditioning and testing in the BBR to confirm if indeed these asphalt binders are of poor quality.

CONTRACT	STIFFNESS (MPa)
J	256.7
K	327.7
L	282
M	345.3

Table 4.3: Stiffness values of the various contracts obtained from BBR testing.

According to the BBR protocol, a stiffness greater than 300MPa is usually associated with poor performing asphalt binders. Contract M which has the highest stiffness value, also has the lowest set of phase angle values (Figure 4.21) while sample J with the lowest stiffness value has a relatively high set of phase angle values (Figure 4.18).

CHAPTER 5

SUMMARY & CONCLUSION

Based on information from preceding chapters, the following conclusion are made:

- Low temperature performance grades of asphalt binders quoted on the mix design reports cannot be completely trusted. EBBR test protocols found that both tank and recovered asphalt binder samples were under-designed for extremely low temperature experienced in-service. Results showed significant deviation from the limiting minimum temperature performance grades quoted in the mix design reports. This is seen to be far worse in recovered samples with some samples being as much as 15⁰C below the expected performance grade. The test also discovered significant difference between the low temperature performance of tank and recovered samples for the same contracts.
- The above finding called for further probing with other performance test like the DENT which again showed some contrast between the performance of tank and recovered samples with regard to fatigue cracking.
- There was therefore the need to consider chemical composition to see if there were some differences in that regard. XRF analysis showed that indeed some modification may have been done on the tank samples after quality assurance tests had been carried out. However, what is actually added to the tank samples prior to road paving is unknown but different amounts of chemical components (heavy metals) in tank and recovered asphalt samples indicate the need for regulatory bodies to further investigate these discrepancies.
- Also, looking at the much-improved high temperature grades of the asphalt binders, it can be concluded that, whatever additives/modifiers are being added to the asphalt mixture before paving seem to have a positive effect on the limiting maximum temperature

performance grade, which implies better resistance to rutting in the recovered samples. However, this improvement is made at the expense of thermal cracking resistance according to data obtained from EBBR.

Based on the findings of this study, it is recommended that regulatory bodies such as the Ministry of Transportation, Ontario (MTO), investigate what happens to asphalt binders at the mix plants, as well as construction sites and to implement stricter quality assurance protocols to ensure there is no inadvertent mixing up of samples.

- Finally, consistency in phase angle trends seen on the black space diagrams for different temperatures and angular frequencies shows much promise for the automated torsion bar experiment as an alternative to the tedious EBBR procedure. Data obtained from phase angle measurements indicate the ability of the procedure to pick up on physical hardening that occurs at extremely low temperatures. However, further study on this test needs to be done in order to validate its efficiency as a test protocol for the predication of thermal cracking in asphalt pavements.

REFERENCES

1. Asphalt Institute, The Asphalt Handbook, Manual Series No. 4 (MS-4), Chapter 1, **1989 Edition.**
2. Asphalt Institute, Superpave Series No. 1 (SP-1), 3rd Edition, Revised **2003.**
3. Material Reference Library Asphalt Data, in Strategic Highway Research Program, National Research Council, Washington, D.C. **1992.**
4. McGennis, R. B., Anderson, R. M., Kennedy, T. W., Solaimanian, M., Background of Superpave Asphalt Mixture Design and Analysis, U.S. Department of Transportation, Federal Highway Administration, Washington, D.C., **1995.**
5. Yildirim, Y., Solaimanian, M. & Kennedy, T.W., Mixing and Compaction Temperatures for Hot Mix Asphalt Concrete (1250-5), **2000.**
6. Wegan, V., Brule, B., “The Structure of Polymer Modified Binders and Corresponding Asphalt Mixtures,” Association of Asphalt Paving Technologists, Vol. 68, **1999.**
7. Traxler, R. N., Asphalt, New York: Reinhold Publishing Corporation, **1961.**
8. Das PK. Ageing of asphalt mixtures: micro-scale and mixture morphology investigation. **2014.**
9. Allen RG, Little DN, Bhasin A., Structural Characterization of Micromechanical Properties in Asphalt Using Atomic Force Microscopy, J. Mater Civil Eng 24(10):1317-27, **2012.**
10. Agbovi, H.K., Effects of Low Temperatures, Repetitive Stresses and Chemical Aging on Thermal and Fatigue Cracking in Asphalt Cement Pavements on Highway 417. thesis, Queen’s University, **2012.**

11. SealMaster Pavement Products and Equipment; http://www.pavemanpro.com/article/deterioration_asphalt_causes/, Accessed: **September, 2016.**
12. Senthil, K.P.; Effects of Warm Mix Additives and Dispersants on Rheological, Aging and Failure Properties of Asphalt Cements. M.Sc. Thesis, Department of Chemistry, Queen's University, Kingston, Ontario, Canada, **2013.**
13. Smith, B. J.; Low-Temperature and Dynamic Fatigue Toughing Mechanisms in Asphalt Mastics and Mixture, MSc. Thesis, Department of Chemistry, Queen's University, Kingston, Ontario, Canada, **2000.**
14. Brown, E. R.; Kandhal, P. S.; Zhang, J.; Performance Testing for Hot Mix Asphalt, National Center for Asphalt Technology, Auburn University, Auburn, **2001.**
15. <https://www.emaze.com/@ALIICZRR/alligator-cracking.pptx>, Accessed: **November 2016.**
16. <http://dottedlinepavement.com/wp-content/uploads/2013/02/waterdamage.jpg>, Accessed: **November 2016.**
17. Orr, D. P.; Pavement Maintenance, Cornell Local Roads Program. 416 Riley-Robb Hall Ithaca, New York, pp. 1-27, **2006.**
18. Kanabar, N.; Comparison of Ethylene Terpolymer, Styrene Butadiene, and Polyphosphoric Acid Type Modifiers for Asphalt Cement, Queen's University Kingston, Ontario, Canada, **2010.**
19. Soleiman, A.; Use of Dynamic Phase Angle and Complex Modulus for The Low Temperature Performance Grading of Asphalt Cement, M.Sc. Thesis, Department of Chemistry, Queen's University, Kingston, Canada, **2009.**
20. <http://www.pavementinteractive.org/article/rutting>, Accessed: **November 2016.**

21. Isacson, U. & Zeng, H., Relationships between bitumen chemistry and low temperature behaviour of asphalt. *Construction and Building Materials*, 11(2), pp.83–91, **1997**.
22. http://www.roadscience.net/sites/default/files/styles/distress_guide_items/public/fatigue%20cracking%202.jpg?itok=5uV4Bu-b, Accessed: **November 2016**.
23. <https://www.fhwa.dot.gov/publications/publicroads/99novdec/images/pave2.jpg>, Accessed: **November 2016**.
24. King, Gayle, et al. Using black space diagrams to predict age-induced cracking, 7th RILEM International Conference on Cracking in Pavements. Springer Netherlands, **2012**.
25. Sowah-kuma, D.; Assessment of Low Temperature Cracking in Asphalt Pavement Mixes and Rheological, M.Sc. Thesis, Department of Chemistry, Queen’s University, Kingston, Canada, **2015**.
26. Jung, D.H., Vinson, T.S.; Low-Temperature Cracking: Test Selection. Strategic Highway Research Program, National Research Council Washington, DC, pp. 14-18, **1994**.
27. Kriz, P., Stastna, J., Zanzotto, L.; Physical Aging in Semi-Crystalline Asphalt Binders. *Journal of the Association of Paving Technologists*, Vol.77, pp. 795-820, **2008**.
28. Anderson, D.A; Dongre, R.; The SHRP Direct Tension Specification Test- Its Development and Use. In: *Physical Properties of Asphalt Cement Binders*, John C. Hardin (Ed), ASTM STP 1241, American Society for Testing and Material, Philadelphia, pp.51- 66, **1995**.
29. Subramani, SK.; Validation of New Asphalt Cement Specification Test Methods using Eastern Northeastern Ontario Contracts and Trial Sections, MSc. Thesis, Department of Chemistry, Queen’s University, Kingston, Ontario, Canada, **2009**.

30. Chen, J. S; Tsai, C. J. Journal of Materials Engineering and Performance, 8(4), 443, **1999.**
31. Omari, I.O., Effects of Two Warm-Mix Additives on Aging, Rheological and Failure Properties of Asphalt Cements, M.Sc. Thesis, Department of Chemistry, Queen's University, Kingston, Canada, **2014.**
32. Pavement Tools Consortium; Pavement Interactive guide, <http://training.ce.washington.edu/PGI/>, Accessed: September **2016.**
33. American Society for Testing and Materials, Annual Book of ASTM Standard, ASTM, Philadelphia, Pennsylvania, **2004.**
34. Laboratory-Pavement Materials; Penetration of Bituminous Materials, School of Civil and Structural Engineering, Nanyang Technological University, **2002.**
35. http://www.civil.uminho.pt/transportinfra/lab_photos/penetration.JPG, Accessed: **November 2016.**
36. American Society for Testing and Materials; Standard Test Method for Softening Point of Bitumen (Ring and Ball Apparatus), D36-95, **2002.**
37. http://www.civil.uminho.pt/transportinfra/lab_photos/ring_ball.JPG, Accessed: **November 2016.**
38. <http://www.priasphalt.com/files/testingandspecifications/astmd21712010091010065433.jpg>, Accessed: **November 2016.**
39. <http://www.pavementinteractive.org/article/rolling-thin-film-oven>, Accessed: **November 2016.**
40. <http://www2.statler.wvu.edu/~wwwasph/pictures/asplab/rtfo.jpg>, Accessed: **November 2016.**

41. Anderson, D.A., Cristensen, D.W., Bahia, H.U., Dongre, R., Sharma, M.G., Antle, C.E., Button, J.; "Binder Characterization and Evaluation, Volume 3." SHRP-A-369, Strategic Highway Research Program, National Research Council, Washington, D.C. **1994.**
42. <http://www.pavementinteractive.org/article/pressure-aging-vessel>, Accessed: **November 2016.**
43. AASHTO M320; Standard Specification for Performance-Graded Asphalt Binder
American Association of State Highway and Transportation Officials, **2002.**
44. Marasteanu M. O.; Basu,A.; Hesp, S. A. M.; Volle, V. International Journal of Pavement Engineering, 5(1), 31, **2004.**
45. Mang, T.; Bituminous materials, University of Florida. Website:
<http://nersp.nerdc.ufl.edu/~tia/Bituminous-Materials.pdf>, Accessed: **October 2016.**
46. <http://www.pavementinteractive.org/article/bending-beam-rheometer>, Accessed:
November 2016.
47. <http://www.slideshare.net/hronaldo10/04superpave-binder-testing-highway-and-airport-engineering-dr-sherif-elbadawy>, Accessed: **November 2016.**
48. US Department of Transportation: Federal Highway Administration; Background of Superpave Asphalt Binder Test Methods, Publication No. FHWA-SA-94-069, **1994.**
49. http://www1.umassd.edu/engineering/cen/materials/equipment/binder/dsr2_small.jpg,
Accessed: **November 2016.**
50. Struik, L. C. E.; Physical Aging in Amorphous Polymers and other Material, Elsevier Scientific Publishing Co. Amsterdam, **1978.**
51. Traxler, R. N.; Schweyer, H. E. Proceedings of the Thirty-Ninth Annual Meeting, American Society for Testing Materials, Atlantic City, NJ, 36(II), 544, **1936.**

52. Traxler, R. N.; Coombs, C. E. Proceedings of the Fortieth Annual Meeting, American Society for Testing Materials, New York City, NY, 37(II), 549, **1937**.
53. Traxler, R. N.; Asphalt – Its Composition, Properties and Uses. Reinhold Publishing, New York, **1961**.
54. Freeston, Jamie-Lee, et al. "Physical Hardening in Asphalt." Proceedings of the Sixtieth Annual Conference of the Canadian Technical Asphalt Association (CTAA): Winnipeg, Manitoba. **2015**.
55. Ministry of Transportation of Ontario; LS-308 – Determination of Performance Grade of Physically Aged Asphalt Cement Using Extended Bending Beam Rheometer (BBR) Method, Revision 24 to Laboratory Testing Manual, **2007**.
56. Ministry of Transportation of Ontario; LS-299 – Determination of Asphalt Cement's Resistance to Ductile Failure Using Double-Edge-Notched Tension Test (DENT), Revision 24 to Laboratory Testing Manual, **2007**.
57. Ministry of Transportation of Ontario; LS-228 – Accelerated Aging of Asphalt Cement Using Modified Pressure Aging Vessel Protocols, Revision 27 to Laboratory Testing Manual, **2012**.
58. Cotterell, B.; Reddel, J. K. International Journal of Fracture, 13(3), 267, **1977**.
59. <http://www.hespresearchgroup.ca/images/news/AASHTO-SOM.jpg>, Accessed: **November 2016**.
60. Andriescu A, Gibson N, Hesp SAM, Qi X, and Youtcheff, JS. Validation of The Essential Work of Fracture Approach to Fatigue Grading of Asphalt Binders. Journal of the Association of Asphalt Paving Technologists, Vol. 75E, pp. 1-37, **2006**.

61. Togunde, O. P.; Low Temperature Investigations on Asphalt Binder Performance – A Case Study on Highway 417 Trial Sections, MSc Thesis, Department of Chemistry, Queen’s University, Kingston, Canada, **2008**.
62. Hesp, S.A.M., Genin, S.N., Scafe, D., Shurvell, H.F., Subramani, S.; Five Year Performance Review of a Northern Ontario Pavement Trial. Proceedings, Canadian Technical Asphalt Association, Moncton, NB, pp. 99-126, **2009**.
63. Kaveh, F., Hesp, S.A.M.; Spectroscopic Analysis of Pressure Aging Vessel Protocols for The Accelerated Laboratory Aging of Asphalt Cements. Proceedings, First Conference of Transportation Research Group of India, Bangalore, India, pp. 11-20, **2011**.
64. Zhao, M.O., Hesp, S.A.M.; Performance Grading of the Lamont, Alberta C-SHRP Pavement Trial Binders. International Journal of Pavement Engineering, Vol. 7(3), pp. 199-211, **2006**.
65. Hesp, S.A.M., Kelli-Anne N. Johnson, Ross G. McEwan, Senthil Kumar Paul Samy, Scott Ritchie, Michaela Thomas; Effect of Ten Commercial Warm Mix Additives on the Quality and Durability of Cold Lake Asphalt Cement. Submitted for Presentation and Publication 93rd Annual Meeting Transportation Research Board, **2014**.
66. http://static.coleparmer.com/large_images/28615_00.jpg, Accessed: **November 2016**.
67. <http://www.pavementinteractive.org/article/dynamic-shear-rheometer>, Accessed: **November 2016**.
68. Hesp, Simon AM, and Herbert F. Shurvell. "X-ray fluorescence detection of waste engine oil residue in asphalt and its effect on cracking in service." International Journal of Pavement Engineering 11.6: 541-553, **2010**.

69. Hesp S.; An Improved Low Temperature Asphalt Binder Specification Method – Final Report, Queen’s University, Kingston, Ontario, Canada, **2004**.
70. Andriescu, A., Gibson, N., Youtcheff, J.S., Qi, X., Hesp, S.A.M., Critical crack tip opening displacement as a fatigue cracking criterion for asphalt mixtures. Proceedings, Sixth International Conference on Maintenance and Rehabilitation of Pavements and Technological Control, E. Santagata (Ed.), MAIREPAV6, Torino, Italy, pp. 252-261, **2009**.
71. Paliukaite, M., M. Verigin, and S. A. M. Hesp. "Double-edge-notched tension testing of asphalt cement for the control of cracking in flexible asphalt pavements." Bituminous Mixtures and Pavements VI: 13, **2015**.
72. Cabrini DelCorro, Failure Property Analysis of Asphalt Cement Samples at an Intermediate Temperature using Double-Edge-Notched Tension (DENT) Testing, **2015**.
73. <http://www.pavementinteractive.org/article/asphalt-modifiers>, Accessed: **November 2016**.
74. Soleimani A, Walsh S, Hesp SAM. “Asphalt Cement Loss Tangent as Surrogate Performance Indicator for Control of Thermal Cracking.” Transportation Research Record: Journal of the Transportation Research Board, 2126, 39-46, **2009**.